Available online at www.sciencedirect.com
SCIENCE DIRECT®
Journal of Chromatography A, 1068 (2005) 31–57
JOURNAL OF CHROMATOGRAPHY A
www.elsevier.com/locate/chroma

Review

Chiral separations by capillary electromigration techniques in nonaqueous media II. Enantioselective nonaqueous capillary electrochromatography

Michael Lämmerhofer*

Christian Doppler Laboratory for Molecular Recognition Materials, Institute of Analytical Chemistry, University of Vienna, Währingerstrasse 38, A-1090 Vienna, Austria

Available online 21 December 2004

Abstract

A review on the advantages, peculiarities, and the potential of enantioselective capillary electrochromatography (CEC) in nonaqueous media is presented. Some fundamentals on CEC with particular focus on enantioselective CEC are discussed. The strategies, concepts, preferentially utilized chiral selectors and column technologies that have been utilized to succeed in highly efficient enantiomer separations by nonaqueous CEC are described thoroughly.

Keywords: Chiral separation; Capillary electromigration technique; Nonaqueous media; Separation mechanism; Chiral recognition; Solvent effects; Chiral selector; Chiral stationary phase; Monolithic column; Packed column; Polysaccharides; Cyclodextrin; Macrocyclic antibiotics; Chiral ion-exchangers

Contents

* Tel.: +43 1 4277 52323; fax: +43 1 4277 9523.
E-mail address: michael.laemmerhofer@univie.ac.at.

0021-9673/$ – see front matter © 2004 Elsevier B.V. All rights reserved.
doi:10.1016/j.chroma.2004.11.092

1. Introduction

Capillary electrochromatography (CEC) [1] is usually characterized as a hybrid technology obtained by mixing of chromatographic and electrophoretic principles. In enantioselective CEC, the capillary accommodates the (chiral) stationary and mobile phase as well as analytes are transported through the capillary column by virtue of electroosmotic flow (EOF) that is generated on the surface of the (chiral) stationary phase. If the solutes are ionized, electrophoretic migration, which may either take place in a co- or counterdirectional way, will contribute to the overall migration velocity. Sometimes an additional pressure gradient is externally applied, a CEC mode that is termed pressure-assisted CEC and has the aim to speed the analysis and stabilize the flow, but partially leads to loss of the favorably flat EOF profile [1]. Accordingly, the observed migration velocity, v_{CEC}, of the analytes in CEC depends on the EOF velocity, v_{eo}, their effective electrophoretic migration velocity, v_{ep}, in pressure-assisted CEC also on the pressurized flow velocity v_{press}, and the purely chromatographic retention factor, k_{LC}, as given by Eq. (1).

$$v_{CEC} = \frac{v_{eo} + v_{ep} + v_{press}}{1 + k_{LC}} \tag{1}$$

While the numerator of this equation, which characterizes the solute transport, is equal for both enantiomers and thus has influence merely on the speed of analysis, the denominator affects both speed of analysis by the magnitude of the chromatographic retention factor and is the only source for enantioselectivity through differences of the retention factors of the both enantiomers. In other words, electrophoretic mobilities are non-selective contributions in view of generating chiral separation [2,3]. However, if a pair of enantiomers need to be resolved from other components in the mixture too, they may positively contribute to the achiral selectivity of the system. In this context, it is noted that the chromatographic retention factor k_{LC} itself may be composed of enantioselective and non-enantioselective contributions to enantiomer separation, as was outlined by a theory developed by Guiochon and co-workers for HPLC enantiomer separation [4]. The former contributions stems from interaction at the active site of the chiral selector (site II) and the latter may originate from adsorption to achiral sites, e.g. at the support (site I). Thus, under linear conditions i.e. infinite dilution the retention factor k_{LC} is obtained as a linear combination of binding affinities at enantioselective sites II ($b_{ij,II}$) and non-enantioselective sites I (b_I) (equal for both enantiomers) weighted by their respective saturation capacities q_I and $q_{ij,II}$ (Eq. (2) [4]). A maximum of enantioselectivity, namely the intrinsic enantioselectivity of the selector (α_{true}), will be just attainable if the non-enantioselective contribution is zero (Eq. (3a)), while with increasing non-enantioselective adsorption that is identical for both enantiomers, the apparent chromatographic enantioselectivity (α_{app}) will decrease (Eq. (3b)).

$$k_1 = \phi(q_I b_I + q_{1,II} b_{1,II}) = \phi(a_I + a_{1,II}) \tag{2}$$

$$\alpha_{true} = \frac{a_{2,II}}{a_{1,II}} \tag{3a}$$

and

$$\alpha_{app} = \frac{a_I + a_{2,II}}{a_I + a_{1,II}} \tag{3b}$$

wherein the subscript 1 and 2 indicate the first and second eluted enantiomer, the sum $a_I + a_{II}$ represents the equilibrium constant and ϕ the phase ratio. From this discussion it becomes evident that minimization of non-enantioselective (often also termed non-specific) interactions is likewise important and successful for optimization of enantiomer separations as the maximization of the difference of binding strengths of the both enantiomers at the enantioselective sites [4]. The primary aqueous CEC mode to which researchers in enantioselective CEC adhered initially appears to impose some restrictions upon the flexibility in this respect, and extension of the mobile phase mode to nonaqueous conditions in CEC certainly expanded the opportunities to succeed in both optimization of intrinsic enantioselectivities and minimization of non-enantioselective interactions being, e.g. of importance for cationic solutes on silica-based CSPs or for lipophilic organic polymer materials (see below).

Like CEC in general, also enantioselective CEC [2,5,6] has gained tremendous popularity in the mid-to-end of the 1990s, due to its potential advantages like (i) higher efficiency than LC (see below), (ii) removal of the selector from the BGE, as opposed to CE, associated with beneficial effect on detection (less interferences, better sensitivity, less problems with MS coupling and ionization suppression), (iii) improved sample loading capacity compared to CE which is supposed to facilitate the analysis of minor enantiomeric impurities through exploitation of high sample loads, and so forth. While it is normally performed with buffered hydroorganic eluents containing a high percentage of ACN, in order to achieve a fast flow, also CEC in nonaqueous media (NACEC) attracted considerable interest in particular for enantiomer separation, because of a few attractive advantages, feasibilities, and peculiarities:

(i) A variety of chiral stationary phases and column packings develop their limiting maximally accessible intrinsic enantioselectivity due to the governing role of polar hydrogen bond and dipole–dipole interactions for analyte–selector association in nonaqueous media, e.g. the typical normal-phase packings such as Pirkle type CSPs [7]. They usually lose enantioselectivity when they are operated with hydroorganic buffer-acetonitrile mixtures typical for conventional CEC. This argument largely applies even to the polysaccharide type CSPs that have in principle two modes of operation: the reversed-phase (RP) and normal-phase (NP) mode. However, the NP mode is normally the more enantioselective one, which was later also proven for NACEC by Zou and co-

workers [8], and thus a reduction of enantiomer separation has to be accepted upon switching from NP to RP mode. The NACEC mode with polar organic solvents (polar organic mode, PO), in particular ACN based eluents, might be a fairly good substitute for the NP mode. To a certain degree, this may also hold for macrocyclic antibiotic CSPs for which it has been shown by HPLC to reach higher enantioselectivities in the nonaqueous polar organic mode and/or complementary enantiorecognition abilities with the distinct mobile phase modes, i.e. RP, PO, and NP mode.

(ii) The system stability may be improved in the NACEC mode as compared to corresponding aqueous conditions. It is well documented in the literature that bubble formation at the end frit (at the transition of the fritted packing and the open capillary segment) is a severe limitation for the robustness of any CEC method. Using the NACEC mode, we experienced less problems with outgassing and bubble formation which may be attributed to the lower solvation capacity of organic solvents for air on the one hand and the generation of lower currents due to the decreased conductivity creating less thermal stress to the system on the other hand.

(iii) In several instances, shorter elution times and faster analysis may be accomplished, as has been reported by, e.g. [9,10].

Hence, NACEC can be regarded as a really valuable complement to enantioselective CEC and capillary electromigration technologies in general. Along this line, the importance of enantioselective NACEC related to all the enantioselective CEC reports is even more significant than corresponding figures for NACE. The percentage of enantioselective NACEC on all the enantioselective CEC contributions cited in the SciFinder Scholar database is typically found in the 4–14% range [11].

2. The meaning of separation factors (α values) in enantioselective capillary electrochromatography

In enantioselective CEC, researchers borrow terminology either from HPLC or CE to characterize the quality of the selectivity of enantiomer separations. The former is meaningful for the separation of neutrals, however, is biased by electrophoretic migration contributions for ionized solutes. This raises the question of the meaning of α-values for ionized compounds, if calculated by chromatographic formalism despite the electrophoretic influence, and under which constraints and conditions they provide a reasonable measure for the chromatographic selectivity.

If ionic solutes are present, k_{CEC}, calculated by common chromatographic formulas, depends on chromatographic retention factor k_{LC}, electroosmotic mobility μ_{eo} and electrophoretic mobility μ_{ep} as given by Eq. (4) [12]

$$k_{CEC} = \frac{t_e - t_0}{t_0} = k_{LC} - \mu_r k_{LC} - \mu_r \quad (4)$$

with t_e and t_0 being the elution time of the solute and neutral non-retained flow marker, respectively, and wherein the reduced mobility μ_r, which is identical for both enantiomers and describes the relative contribution of electrophoretic mobility to the sum of both driving forces μ_{ep} and μ_{eo}, is according to Schwer and Kenndler [13] defined as

$$\mu_r = \frac{\mu_{ep}}{\mu_{ep} + \mu_{eo}} \quad (5)$$

Thereby, k_{CEC} has the meaning of a peak locator only which specifies the position of the solute peak relative to the EOF marker. The retention window for the separation in CEC involving electrophoretic migration is thus spanned by

$$-1 < k_{CEC} < \infty \quad (6)$$

Separation factors α_{CEC} are then expressed as the ratio of the retention factors of the second and first eluted enantiomers (Eq. (7)).

$$\alpha_{CEC} = \frac{k_{LC,2} - \mu_r k_{LC,2} - \mu_r}{k_{LC,1} - \mu_r k_{LC,1} - \mu_r} \quad (7)$$

They contain the influence of the electrophoretic mobility contribution, which depending on its relative magnitude exerts an alteration on the calculated separation factor α_{CEC}. Though, it is emphasized once more that the electrophoretic mobilities are non-enantioselective contributions in view of generating chiral separation. Four distinct scenarios have been simulated and the results are shown in Fig. 1. The dependencies of α_{CEC} on the electrophoretic velocity contribution v_{ep} is plotted for three different EOF strengths v_{eo} for both co- and counterdirectional separation modes as well as two distinct levels of chromatographic retention factors k_{LC}, i.e. low k ($k_1 = 1$, $k_2 = 2$) and high k ($k_1 = 10$, $k_2 = 20$). Hence the purely chromatographic selectivity α_{LC} which would result from a pressure-driven HPLC experiment is in all cases identical ($\alpha_{LC} = 2$). Fig. 1a and b shows the selectivity variations for a codirectional separation process and Fig. 1c and d for a counterdirectional separation. The findings can be briefly summarized as follows: (i) when the electrophoretic mobility is in opposite direction to the EOF, α_{CEC} declines with increasing importance of the electrophoretic mobility contribution and the slope for the decrease is steeper, if the EOF is weak (Fig. 1c and d). (ii) Minor deviations of α_{CEC} from α_{LC} will be obtained for the highly retentive separation modes ($k_1 = 10$, $k_2 = 20$) when the EOF is moderate ($v_{eo} = 1$ mm/s) to strong EOF ($v_{eo} = 2$ mm/s). This deviation is negative in case of the counterdirectional mode (Fig. 1d) and slightly positive for the codirectional separation (Fig. 1b). For such conditions, α_{CEC} provides a fairly good measure of the liquid chromatographic separation factor. In all other instances, k_{CEC} is meaningless to characterize the chromatographic selectivity. (iii) If the electroosmotic mobility of the system is low, e.g.

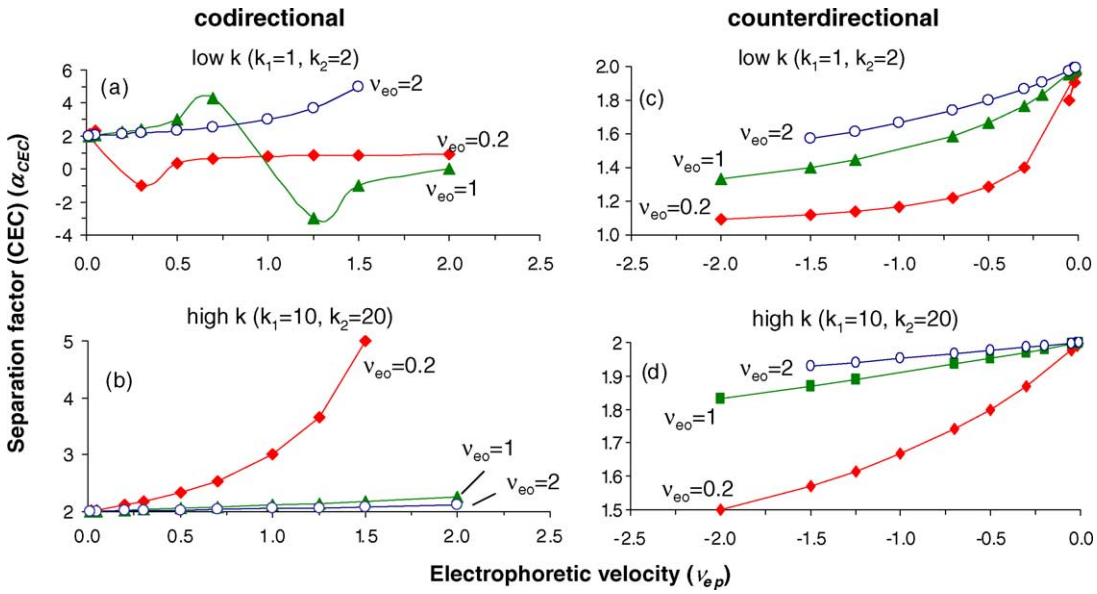

Fig. 1. Simulation of alterations of CEC separation factors α_{CEC} as function of the magnitude of the electrophoretic migration contribution (v_{ep}) (mm/s) of the analyte for three distinct EOF velocities (v_{eo}) (mm/s), i.e. fast, intermediate and slow EOF velocity. (a) Codirectional separation and low retention. (b) Codirectional separation and high retention. (c) Counterdirectional separation and low retention. (d) Counterdirectional separation and high retention. The negative sign of v_{ep} indicates the opposite electrophoretic migration direction of the solute relative to the EOF.

v_{eo} = 0.2 mm/s, and/or the magnitude of the chromatographic retention factors is low, a dramatic decrease of α_{CEC} will be observed in the counterdirectional modes (Fig. 1c and d). (iv) An exceptional increase of α_{CEC} will result from increasingly accelerated electrophoretic migration of the solute in a codirectional separation with low EOF speed (v_{eo} = 0.2 mm/s) and high retention factors (Fig. 1b). (v) In case of low retention and codirectional separation, relatively meaningful values of α_{CEC} will solely be obtained at high EOF speed and low electrophoretic contributions. Otherwise, obscure numbers may be attained and α_{CEC} may adopt even negative values if one enantiomer is eluted before and the other after the neutral marker.

Thus, if the solutes elute very close to or even before the EOF marker the chromatographic terminology to calculate separation factors is meaningless and inappropriate, and the electrophoretic terminology, where α_{CE} is calculated as the ratio of the mobilities or linear velocities or simply elution times seems to be preferred.

$$\alpha_{CE} = \frac{v_{CEC,1}}{v_{CEC,2}} = \frac{1 + k_{LC,2}}{1 + k_{LC,1}} \quad (8)$$

According to Eq. (8) this terminology suggests to be free of electrophoretic bias. The separation factors calculated by this way are therefore independent of electrophoretic mobility and electroosmotic flow and depend solely on the chromatographic retention factors. However, they are always lower than the liquid chromatographic separation factors. The degree being lower than α_{LC} depends on the magnitude of k_{LC} relative to unity. At $k_{LC} > 10$ the deviation between separation factors calculated by the ratio of migration velocities of first and second eluted enantiomer α_{CE} and α_{LC} becomes small. For example, α_{CE} values of 1.50 (Fig. 1a and c) and 1.91 (Fig. 1b and d) have been calculated by Eq. (8) for low and high k scenarios, respectively, regardless of the magnitudes of electroosmotic and electrophoretic mobility contributions, while the chromatographic separation factor α_{LC} value would always be 2.0, as mentioned above.

3. Solvent effects

Like in any CEC method, a high EOF is of utmost importance also in enantioselective NACEC from the viewpoint of a fast analysis and a stable system. Since the dielectric/viscosity ratio is supposed to be the governing factor of the medium for a strong EOF, *N*-methylformamide (NMF) and acetonitrile (ACN) would be the solvents of first choice. In fact, however, in most enantioselective NACEC studies mixtures of solvents in particular of ACN and MeOH have been employed. NMF has practically no importance in NACEC yet and also other solvents were due to lack of high EOF employed seldom. In practice it turned out that the EOF behavior cannot be predicted firmly from the ε/η ratio. The theory of electroosmotic flow in CEC is much more complex [14]. The complexity arises mainly from the presence of the packing and the duplex geometry of the columns with packed and open segments, inhomogeneities of the packing, heterogeneities of the ζ-potential, e.g. mismatch of ζ-potential of packings and FS wall, and so forth. Thus, the effect of a variety of factors is difficult to forecast and may be responsible for deviations from the expected behavior in NACEC experi-

ments. Such hardly forseeable effects imposed upon a solvent exchange include, for example:

(i) Variations of the ionic compositions of the eluent (even when the same amount of electrolyte is added) originating from different dissociation and protonation, respectively, and conjugation or association of ionic species.
(ii) Changes of the stationary phase surface in particular of the ζ-potential (see Eq. (9)) caused by the solvent exchange. The ζ-potential itself depends on the medium [13].

$$\zeta = \frac{\sigma\delta}{\varepsilon_0\varepsilon_r} \quad \text{and} \quad \delta = \sqrt{\frac{\varepsilon_0\varepsilon_r RT}{2F^2 I}} \tag{9}$$

wherein σ is the surface charge of the chiral stationary phase, δ the double layer thickness, R the gas constant, T the absolute temperature, F the Faraday constant, and I is the ionic strength of the eluent.
Moreover, distinct solvents may influence adsorption of ionic species to a different degree. Altered protonation equilibria in distinct media (pK and pH* shifts) may vary the actual surface charge and ζ-potential, respectively. Ion-pairing between oppositely charged ionic groups of the stationary phase and the eluent thereby also reducing the actual ζ-potential may occur to different extent owing to the dielectric constant of the medium (many of the electrolyte components used in NACEC exhibit ion-pair properties, e.g. acetic acid, triethylamine, etc.).
(iii) Changes of the porous properties of the packing and chromatographic bed, respectively. This applies in particular, for example, to organic polymer monoliths with low crosslinking. Swelling and shrinkage upon solvent exchange may alter the effective macropore and mesopore diameters [15], and it has been shown that the EOF velocity depends on the macropore diameter [16].
(iv) Double layer overlaps in the intraparticulate pore channels, which lead to decrease of the overall flow velocity and loss of favorable flow profile, may emerge to different extent in distinct media.

Due to a still limited understanding of all these factors in nonaqueous solvents at present experimentation beyond the common with the goal of EOF optimization is therefore worthwhile in NACEC. For example, unexpected EOF behavior in enantioselective NACEC was reported by several authors [10,17]. For example, Tobler et al. found a maximum EOF velocity with a mixture of MeOH–ACN (60:40, v/v), while both mixtures with higher MeOH and ACN content, as well, yielded lower flow rates.

As electrolytes, acetic acid, formic acid, MES, ammonia, triethylamine have been commonly employed in enantioselective NACEC, but also the electrolyte-free NACEC approach was reported recently, e.g. by Vickers and Smith [7]. In this study, the normal-phase mode was tested for enantiomer separation by a Pirkle-type CSP (Whelk-O 1). Since electrolytes lack solubility, the addition of 1 or 5% (v/v) water was considered instead to achieve sufficient conductivity and EOF. Clearly with higher water content in the hexane-2-propanol (2-PrOH) (1:1, v/v) mixture, the EOF velocity increased, but showed a leveling effect already at a water content of about 3% (v/v). EOF velocities of about 0.1 mm/s only without supporting hydrodynamic flow could be reached. The application of an additional pressurized flow favorably supported the speed of elution, while with 5% (v/v) water there was still NP character maintained. A number of solutes could be resolved into individual enantiomers and it was clearly demonstrated (i) that R_S was higher with 5% (v/v) water and faster with this percentage and (ii) the mode with CEC and external pressure (CEC + P) outperformed either of the parent technologies alone (Fig. 2). As mentioned above an NP-like mode was also evaluated by Chen et al. [8] who used the hexane-based eluent together with alcohols, THF and acetic acid–triethylamine as electrolytes, e.g. a typical mobile phase consisted of hexane–MeOH–2-PrOH–THF (50:35:10:5, v/v/v/v) and 5 mM acetic acid–triethylamine.

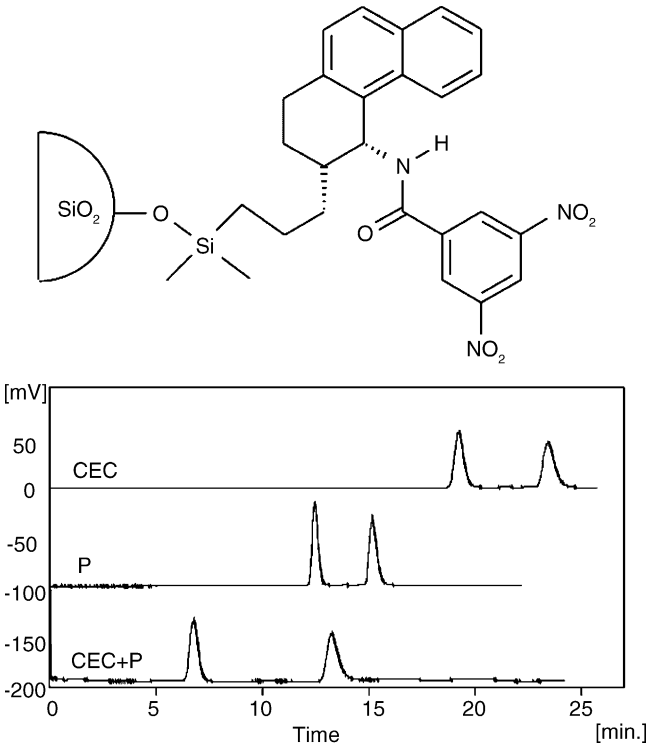

Fig. 2. Chromatograms showing the separation of the chiral analyte benzoin by CEC, pressure (P), and pressure-assisted CEC (CEC + P). Mobile phase: hexane–2-PrOH (1:1, v/v) +5% (v/v) water. CSP: Whelk O-1. Reprinted with permission from ref. [7].

EOF is inherently connected to the intrinsic systems parameters mobile phase, stationary phase and column packing. On the other hand, achieving satisfactory enantioselectivity is extremely critical and strongly solvent depending in enantiomer separation. As a consequence, EOF speed is thus mostly regarded of secondary relevance and importance and may often be sacrificed in favor of enantioselectivity, if the selectivity tuning does require. Hence, EOF velocity is typically

a compromise in enantiomer separation. Indeed, for example, polysaccharide CSPs are run in NACEC typically with purely methanolic eluents and, e.g. also macrocyclic antibiotics are operated with suboptimal solvents in terms of EOF speed.

Solvent effects on electrophoretic mobilities and selector–analyte interactions are governed by the same principles as described for NACE (part 1 of this review [11]).

4. Modes of enantioselective nonaqueous capillary electrochromatography and column technologies

Enantioselective CEC has been carried out either in the 'additive mode' or the 'CSP approach'. For the latter, three different column technologies have been proposed [2Lämmerhofer, 2000 #167, 5, 6]: (i) open-tubular columns (with dynamically adsorbed selectors, coated polymeric selectors, or covalently linked brush-like selectors), (ii) packed columns (densely filled with conventional silica-based microparticulate CSPs), (iii) organic polymer or silica monolith columns (with selectors either incorporated by in situ copolymerization of a chiral monomer or attached by derivatization of the reactive monolithic support). The advantages and drawbacks of each of these column technologies have been described in detail in various reviews and monographs on CEC [1]. Of practical relevance for enantioselective NACEC are solely the both latter technologies, while no reports with open-tubular capillary columns in the NACEC mode have been published up to now. This may be related to the low phase ratio of open-tubular columns and a low saturation capacity of enantioselective sites originating from a small surface area of the FS wall. Both together with the weakening of the strength of many interactions like hydrophobic interactions, in nonaqueous solvents make the adsorption too weak with polar organic eluents. Also other disfavorable properties of the open-tubular column approach such as ease of overloading, susceptibility for clogging in the course of their synthesis, need for very narrow capillary diameters to achieve reasonable efficiency which is then accompanied by detection insensitivity, all may have contributed that this approach has not become accepted in the field of NACEC. The enantioselective NACEC studies that have been reported using either packed or monolithic columns are summarized in Table 1 and will be discussed in the following chapters. However, a few general aspects are already outlined beforehand.

Most CEC columns, packed and monolithic as well, possess a duplex geometry with a packed and an open segment. Since the conductivities in the open and packed segments are different, the electric field does not drop uniformly through the column, but different electric field strengths are imposed on the two distinct sections [14]. Owing to tortuous flow channels through the packed or monolithic bed, analyte and mobile phase must travel a longer path than the effective length of the capillary (from injector to detector). When parameters with physicochemical meaning such as the actual electroosmotic mobility of the neutral marker in the packed segment, $\mu_{eo,packed}$, are to be derived from a CEC run, this has to be considered and actual voltage drop and the length of the tortuous flow channel have to be used for the calculations [14].

The columns packed with microparticulate chiral stationary phase are extremely vulnerable and susceptible for several problems. The retaining frits that keep the packing in place during the run are usually directly sintered on the CSPs. The chiral organic surface modification of the functionalized silica particles disfavor the fusion of the silica spheres, which therefore requires sometimes harsh conditions. Such conditions of course destroy both the organic chiral surface modification and the external protective polyimide layer of the capillary where the capillary thus becomes fragile. The fritted region represents another discontinuity and inhomogeneity (in addition to the open bed) where the ζ-potential, the conductivity and (electrokinetic) permeability are altered. Altogether may have a detrimental effect on the chromatographic efficiencies that can be achieved. Moreover, the end frit is fragile and is the place, where onset of bubble formation typically occurs, which severely hampers the system stability and robustness of CEC with packed columns.

The theoretical plate numbers that can be obtained by CEC are typically in the range between HPLC (low end) and CE (high end). The enhanced efficiency in CEC as compared to HPLC stems mainly from three factors: (i) flatter profile of EOF compared to parabolic hydrodynamic flow, (ii) smaller particle diameters typically 3 or 3.5 μm rather than 5 μm (or equivalent smaller sphere diameter of the polymer globules and skeletons, respectively, in monolithic columns) provide shorter path lengths for diffusive intraparticle mass transfer and less flow dispersion which both translate into smaller A-term (flow maldistribution) and lower C-term (resistance to mass transfer) contributions to band spreading. In addition, the independence from pressure drop allows the use of longer packed columns (typically 25 cm) with small diameter particles, which is associated with an aliquot improvement of the plate number. (iii) Since the EOF is generated directly on the surface of the stationary phase anywhere in the chromatographic bed, mobile phase propulsion within the intraparticle pore channels can be accomplished in wide pore materials and the resulting intraparticulate convective mass transfer reduces inequalities of inter- and intra-particle flow patterns [18]. Wide pore materials have been shown to be favorable for the generation of a strong perfusive intraparticle flow that enhances mass transfer [19]. In contrast, excessive double layer overlap in narrow pores (e.g. if the double layer thickness is large relative to the diameter of the flow channel, e.g. $d_{channel}/\delta < 10$) may lead to partial loss of the intraparticle pore flow velocity and also of the favorable flat profile.

Unfortunately, 3 μm particles were until recently only available with typical mesopore size of 100 Å so that a strong convective intraparticle flow and mass transfer was hardly to exploit with such materials. However, 3 μm particles seem to become now available as 200 Å material, e.g. from

Table 1
NACEC enantiomer separations using chiral stationary phases (CSPs)

Selector/CSP	Column type	Solvent/eluent	Electrolytes	Compounds	N/m ($\times 10^3$)	Referennce
Coated polymeric selectors						
Poly(diphenyl-2-pyridylmethylmethacrylate) coated on aminopropylsilica (APS) 5 μm (1000 Å)	Packed (100 μm i.d.)	MeOH	2.5 mM ammonium acetate (NH_4Ac) pH^* 4.5	Benzoin derivatives, 1,1′-binaphthyl-2,2′-diol, trans-stilbene oxide	Up to 27	[17,27]
Chiralpak AD (16%, w/w) and Chiralcel OD (4%, w/w) (coated on wide bore APS)	Packed (100 μm i.d.)	MeOH–EtOH (75:25, v/v)	2.5 mM ammonium acetate	Thalidomide and its hydroxylated metabolites		[28]
Chiralpak AD, Chiralcel OD, Chiralcel OJ coated on APS (3 and 5 μm) (60–2000 Å)	Packed (100 μm i.d.)	MeOH, EtOH	2.5–10 mM ammonium acetate	Piprozolin, trans-stilbene oxide, gluthethimide, indapamide, aminoglutethimide, Troeger base, thalidomide, nifurtimox	Up to 176	[29–31]
Cellulose tris(3,5-dichlorophenylcarbamate) coated on silica 1000 Å, 5 μm	Packed (100 μm i.d.)	MeOH	15 mM ammonium acetate	Ambucetamide, benzyl 2-(benzylsulfinyl)benzoate, etozolin, norgestrel, omeprazole, piprozolin, thalidomide	240	[32]
Cellulose tris(3,5-dichlorophenylcarbamate) coated on APS 2000 Å, 5 μm	Packed (100 μm i.d.)	MeOH	2.5 mM ammonium acetate	Benzyl 2-(benzylsulfinyl)benzoate, 2-(benzylsulfinyl)benzamide, etozolin, piprozolin	215	[33]
Cellulose tris(3,5-dichlorophenylcarbamate) coated on APS 60–2000 Å, 5 μm	Packed (100 μm i.d.)	MeOH	2.5 mM ammonium acetate	Piprozolin	400	[34,35]
Covalently bonded polymeric selectors						
Cellulose 2,3-O,O-bis(phenylcarbamate) immobilized in 6-O-position via 4,4′-diphenylmethane diisocyanate spacer to APS 5 μm, 300 Å	Packed (100 μm i.d.)	Hexane–MeOH–2–PrOH–THF (60:25:10:5, v/v)	5 mM acetic acid–triethylamine	Warfarin, praziquantel	Up to 80	[8]
Cellulose 2,3-O,O-bis(phenylcarbamate) and cellulose 2,3-O,O-bis(3,5-dimethylphenylcarbamate) immobilized in 6-O-position via toluene-2,4-diisocyanate spacer to diethylenetriaminopropylsilica 5 μm, 200 Å	Packed (100 μm i.d.)	EtOH or Hexane–MeOH–EtOH (35:25:8, v/v)	14.2 mM acetic acid, 1.4 mM DEA	Troeger base, praziquantel, benzoin, trans-stilbene oxide	Up to 35	[36]
Cellulose 2,3-O,O-bis(phenylcarbamate)-6-O-methacryloyl copolymerized with methacryloyl-modified diethylenetriaminopropylsilica 5 μm, 200 Å	Packed (100 μm i.d.)	35–50% (v/v) EtOH in hexane	14.2 mM Acetic acid, 1.4 mM DEA	Troeger base, praziquantel, benzoin, warfarin, propranolol, metoprolol, ranolazine	20	[37]
Macrocyclic selectors with inclusion complexation abilities						
β-CD, γ-CD attached to silica via carbamate linker (ChiraDex-beta 3 μm, ChiraDex-gamma 5 μm)	Packed (100 μm i.d.)	MeOH, 30–70% (v/v) ACN in MeOH	10 mM MES	Dns-amino acids	70–125	[9]
Vancomycin, immobilized to pre-packed diol silica (5 μm) columns via three-step procedure	Packed (75 μm i.d.)	MeOH–ACN	AcOH–TEA (0.1–0.6% each, v/v)	Thalidomide, β-blockers	45–120	[38]
Vancomycin (5 μm Chirobiotic V)	Packed (75 μm i.d.)	15–20% (v/v) ACN in MeOH	AcOH–TEA (0.1:0.1, v/v)	Thalidomide, β-blockers, terbutaline	30–190	[39]
Vancomycin-CSP	Fully packed (50, 75 μm i.d.) with three segments (diol-silica in frit and detection segments)	MeOH, MeOH–ACN (var.%), EtOH, *n*-PrOH, 2-PrOH	13 mM ammonium acetate	Basic compounds including β-blockers, β-sympathomimetics, antidepressants	50–80	[40]
Teicoplanin (5 μm Chirobiotic T)	Packed (75 μm i.d.)	5–20% (v/v) ACN in MeOH	Acetic acid–TEA (0.05–0.3% each, v/v)	Basic drugs (amino alcohols)	30–137	[41]
Teicoplanin (5 and 3 μm Chirobiotic T)	Packed (75 μm i.d.)	5% (v/v) ACN in MeOH	AcOH–TEA (0.05:0.05, v/v)	Metoprolol, alprenolol and other β-blockers	80 and 260, respectively	[42]

Table 1 (*Continued*)

Selector/CSP	Column type	Solvent/eluent	Electrolytes	Compounds	N/m ($\times 10^3$)	Referennce
Teicoplanin (3.5 and 5 μm) and teicoplanin:silica (3:1, w/w)	Fully packed (75 μm i.d.) with three segments (diol-silica in frit and detection segments)	40% (v/v) ACN in MeOH	0.05% (w/v) ammonium acetate	Basic compounds viz. amino alcohols (β-blockers, β-sympathomimetics) and antidepressants	35–210	[20]
Teicoplanin aglycone (Chirobiotic TAG) (on 3.5 μm silica)	Packed (100 μm i.d.)	10–20% (v/v) ACN in MeOH	AcOH–TEA (0.2:0.2, v/v)	amino alcohols (β-blockers, β-sympathomimetics) and few other drugs	Up to 65	[43]
Chiral anion exchangers						
O-*tert*-butylcarbamoyl quinine (tBuCQN) covalently bonded to 3-mercaptopropylsilica (TPS) (3.5 μm, 100 Å)	Packed (100 μm i.d.)	MeOH, MeOH–ACN (var. ratios)	AcOH–TEA (var. conc.)	FMOC, DNZ, Z, Bz, Ac, DNP-amino acids, dichlorprop, etodolac	100	[10]
tBuCQN-TPS (3.5 μm, 100 Å)	Packed (100 μm i.d.)	MeOH–ACN (20:80, v/v)	400 mM AcOH, 4 mM TEA	Atropisomeric 2′-dodecyloxy-6-nitrobiphenyl-2-carboxylic acid	150	[44]
Poly{O-[2-(methacryloyloxy)ethylcarbamoyl]-10,11-dihydroquinidine-co-HEMA-co-EDMA}	In situ monolithic (100 μm i.d.)	MeOH, MeOH–ACN (var. ratios)	AcOH–TEA (var. conc.)	DNB, FMOC, DNZ, Z, Bz, Ac, DNP-amino acids, mecoprop, fenoprop	240	[45–47]
Poly{O-9-*tert*-butylcarbamoyl)-11-[2-(methacryloyloxy)ethylthio]-10,11-dihydroquinine-co-HEMA-co-EDMA}	In situ monolithic (100 μm i.d.)	MeOH–ACN (20:80, v/v)	400 mM AcOH, 4 mM TEA	DNB, DNZ, FMOC, CC, DNS, DBD-amino acids	200	[48]
Poly(GMA-co-EDMA) derivatized with tBuCQN	Post-mod. monolithic (100 μm i.d.)	MeOH–ACN (20:80, v/v)	400 mM AcOH, 4 mM TEA	DNB-Leu	57	[49]
Chiral cation exchangers						
N-(4-Allyloxy-3,5-dichlorobenzoyl)-1-amino-3-methylbutanephosphonic acid and *N*-(3,5-dichlorobenzoyl)-O-allyl-tyrosine bonded to TPS (3.5 μm, 100 Å)	Packed (100 μm i.d.)	MeOH, MeOH–ACN (var. ratios)	AcOH–TEA (var. conc.)	Amino alcohols (β-blockers, β-sympathomimetics, antimalaria agents), oxyphencyclimine, etidocaine, promethazine	50–360	[50]
N-(4-Allyloxy-DCB)-2-amino-3,3-dimethylbutanesulfonic, phosphonic acid and corresp. carboxylic acid bonded to TPS (3.5 μm, 100 Å)	Packed (100 μm i.d.)	MeOH–ACN	2-Aminobutanol, formic acid	Amino alcohols (β-blockers, β-sympathomimetics, antimalaria agents), phenmetrazine, benzetimide, omeprazole	Up to 300	[51]
N-(4-Allyloxy-DCB)-cysteic acid, penicillamine sulfonic acid, *tert*-butylamido penicillamine sulfonic acid, $CySO_3H$-Leu bonded to TPS (3.5 μm, 100 Å)	Packed (100 μm i.d.)	MeOH–ACN (20:80, v/v)	2-Aminobutanol, formic acid	Amino alcohols (β-blockers, β-sympathomimetics, antimalaria agents), flecainide, benzetimide	Up to 300	[52]
N-(4-Allyloxy-DCB)-*tert*-butylamido penicillamine sulfonic acid bonded to TPS (3.5 μm, 100 Å)	Packed (100 μm i.d.)	MeOH–ACN (20:80, v/v)	25 mM 2-aminobutanol, 50 mM formic acid	Ephedrine	320	[53]
N-(4-Allyloxy-DCB)-sulfodipeptides bonded to TPS (3.5 μm, 100 Å) (DCB = 3,5-dichlorobenzoyl)		MeOH–ACN (20:80, v/v)	25 mM 2-aminobutanol, 50 mM formic acid	Amino alcohols (β-blockers, β-sympathomimetics, antimalaria agents), flecainide, benzetimide, omeprazole		[54]

Kromasil, which could provide even better flow and performance characteristics. Due to independence from the pressure drop it could be shown that 3 μm particles could afford even a higher EOF velocity than a corresponding 5 μm particulate material [20,21]. This behavior might result from the higher surface-to-volume ratio of the former at a comparable surface density of ionic groups.

In enantioselective NACEC solely organic polymer based monoliths have been utilized, while silica monoliths were not yet explored by this technique. This general discussion is therefore restricted to the organic polymer monolithic columns. The simple column fabrication from (acrylamide or methacrylate) monomer solutions that are filled into the capillary, which usually has prior been vinyl-modified to allow a crosslinking and immobilization of the monolithic structure to the capillary wall, makes this column technology attractive compared to the packed columns. Hence, columns with a fritless design are obtained, which of course overcome frit-related problems such as strong propensity for bubble formation and poor column stability. Chemistry and pore properties can be flexibly tailored. The former allows the copolymerization of an ionizable monomer for EOF generation and a chiral monomer for the chromatographic partitioning. The latter can be adjusted by an appropriate choice of porogens (rigid polymethacrylate monoliths) or concentration of salt (polyacrylamide monoliths) in the polymerization mixture [16,22]. Typically, there is a trend that macroporous organic polymer monoliths with larger through-pore diameters (wider flow channels) are accompanied by larger-sized polymer globules. Yet, in sharp distinction to the above described relationship between EOF velocities and particle diameter of packed columns, the electroosmotic mobility of organic polymer monolith columns, in particular of the rigid organic polymethacrylate type monoliths, increases with the diameter of the flow-through pores. This behavior is somehow in contradiction to the common perception of CEC theory that the electroosmotic mobility is independent of the flow channels. This unexpected behavior was explained by Svec and co-workers to originate from microscopic variations in field strength, tortuosity, and conductance in small and large diameter monolith columns. In such monoliths it is common understanding that the flow through the macropores is largely convective. Whether meso and micropores are available and to what extent convective and/or diffusive mass transfer in these narrower pores contribute to the dynamics of low molecular analytes in CEC is not very well studied yet [23]. In any case, the morphology of the monoliths determines both flow properties and efficiency strongly and requires a careful adjustment, in order to achieve highly efficient separations. More details on monolith fabrication and properties can be found elsewhere [16,22].

Besides ‘CSP approaches’ also the ‘additive mode’ with selector (*tert*-butylcarbamoylquinine) added to the nonaqueous mobile phase and the use of an achiral stationary phase (Hypersil C18-3 μm) was successfully realized [24].

The additive mode is a simple option to achieve enantiomer separations using commercially available capillary columns with achiral packings (e.g. reversed-phase columns). In this case, selector–selectand association takes place in the mobile phase and/or on the stationary phase, if the chiral selector molecules get adsorbed onto the stationary phase, thus generating, controlled by secondary equilibria, a dynamic coating. The capillary format makes this technique attractive and affordable, since selector consumption is low due to the small internal volume of the capillary column. Advantages of CEC using the CSP approach in comparison to CE (‘additive mode’) like elimination of the selector from the BGE, the detector cell, and the effluent are lost when the additive mode is utilized and no other real advantages become apparent. Hence this technique possesses no real practical relevance.

While this approach is very simple from the practical viewpoint, the separation mechanism in this technique may be rather complex. The separation selectivity between enantiomers arises as a result of: (i) the difference in the equilibrium constants of complex formation of (R) and (S) enantiomers with the chiral selector (intrinsic selectivity); (ii) the mobility difference of the diastereomeric selector–analyte associates formed in the mobile phase; (iii) the concentration of the selector in the BGE and/or adsorbed onto the stationary phase; (iv) the mobility difference of the free and complexed solute; (v) the differential partitioning of the diastereomeric selector–analyte associates; (vi) the differential partitioning of free and complexed enantiomers onto the stationary phase.

Overall, this CEC methodology in the additive mode is very similar to CE from both the practical viewpoint, but also mechanistically (cf. reversal of elution orders as response of a change of the relative magnitude of EOF and electrophoretic migration [24–26]), and a benefit over CE is hard to reason.

In the following, the various reported ‘CSP approaches’ that have utilized nonaqueous conditions including both packed as well as monolithic columns will be discussed together with their specifics in NACEC. Mainly, three distinct classes of selectors and corresponding CSPs gained importance for enantioselective NACEC: (i) synthetic or semisynthetic polymeric selectors, in particular polysaccharide based CSPs, (ii) macrocyclic selectors including cyclodextrins and antibiotics phases, and (iii) chiral ion exchangers including both anion as well as cation exchangers.

5. Selectors and chiral stationary phases in nonaqueous capillary electrochromatography

5.1. Polymeric selectors

One of the first studies on enantioselective NACEC explored a CSP obtained by coating synthetic helically chiral poly(diphenyl-2-pyridylmethyl methacrylate) (Fig. 3) as selector onto unmodified and aminopropyl-modified wide-pore silica (5 μm) materials [17,27]. This selector, which is synthe-

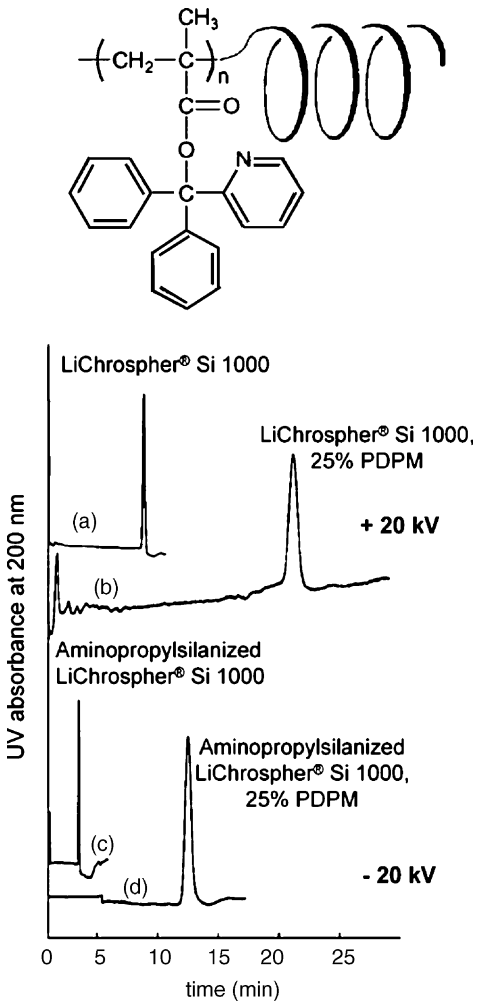

Fig. 3. Polymeric poly(diphenyl-2-pyridylmethylmethacrylate) CSP used in enantioselective NACEC and its EOF behavior upon coating of the selector (25%, w/w) onto silica and aminopropylsilica 1000 Å, 5 μm. EOF marker, thiourea. Eluent, 2.5 mM ammonium acetate in MeOH. Reprinted with permission from ref. [17].

sized from achiral monomers and adopts its chirality through ordered superstructure and helical arrangement of the polymer chain, was known to resolve enantiomers in pure MeOH and therefore selected for these pioneering works. A variety of parameters have been studied systematically. For example, the type of silica used for coating of the selector was investigated as function of pH* with regards to EOF generation [17]. It was found that the aminopropylsilica particles showed a higher EOF with the employed methanolic eluent (2.5 mM ammonium acetate) than the corresponding native 1000 Å wide-pore silica at almost any pH*, but in particular at acidic conditions. Suppression of silanol ionization at low pH with the silica material and a high amino group density of the aminopropylsilica, positively charged at such conditions, conveniently explain this comparative behavior. Moreover, the flow of the 3-aminopropylsilica (APS) particles was due to the dominance of the amino groups over the residual silanols anodic and reached a maximal mobility at pH* 6. The electroosmotic mobilities ranged between $-8 \times 10^{-5}\ V^{-1}\ s^{-1}$ and $-15 \times 10^{-5}\ V^{-1}\ s^{-1}$. The lower EOF at higher pH* may readily be explained by the dissociation characteristics of the primary amine and the counteracting effect of the silanols which are increasingly deprotonated and become an important contribution to net charge and EOF generation. In contrast, the decrease of EOF at pH* < 6 most likely originated from the addition of acetic acid for pH* adjustment and concomitant increase of the ionic strength of the medium which slowed down the EOF.

A densely coated layer of neutral polymer onto the surface of ionizable particles may function like an insulator for the charges beneath the surface. This way, through coating of 25% (w/w) of the polymeric selector onto the surface of the wide-pore materials the EOF was dramatically diminished in both cases, unmodified silica and aminopropylsilica as well. The relative decrease was found to be even higher for the APS material (4.7-fold compared to 2.6-fold for silica) (see Fig. 3). Indirectly, it was concluded that the pyridyl groups do not serve as source for EOF generation. This adverse shielding effect and ensuing EOF reduction of the coated layer is specific and intrinsic for the adsorptively coated polymer CSPs.

As already mentionend above, unexpected solvent dependence of the EOF was observed in this study. In contradiction to the ε/η ratio, a faster EOF was delivered by MeOH than ACN, and even the ACN–water (90:10, v/v) mixture revealed only slightly higher EOF velocity than MeOH. Chiral compounds such as benzoin derivatives and trans-stilbene oxide could be resolved in methanolic BGE and the addition of water had a favorable influence on the resolution, but significantly impaired separation speed.

Overall this type of selector that is certainly of high scientific interest due to its intriguing structure has only a limited scope of application in enantioselective NACEC and moderate relevance. Moreover, problems such as partial loss of the helical structure may occur if inappropriately operated.

Besides this CSP based on entirely synthetic polymeric selector, particulate materials modified with semisynthetic polysaccharide derivatives have been thoroughly studied in enantioselective NACEC [8,28–37,55]. This is not further surprising, because polysaccharide derivatives represent the most broadly applicable class of chiral selectors in HPLC enantiomer separation. A thorough review describing the characteristics and peculiarities of these CSPs in enantioselective NACEC has been published recently [56].

Of the variety of different variants of polysaccharide CSPs the NACEC potential of the most common ones, i.e. cellulose tris(3,5-dimethylphenylcarbamate) (known as Chiralcel OD) [28–31], amylose tris(3,5-dimethylphenylcarbamate) (Chiralpak AD) [28–30], cellulose tris(4-methylbenzoate) (Chiralcel OJ) [29] and the more uncommon cellulose tris(3,5-dichlorophenylcarbamate) [32,34,35] has so far been elucidated (for structures see Fig. 4). Type of polysaccharide (i.e. cellulose or amylose), distinct substitution pattern, and supramolecular structure of the coated polymer layer, which

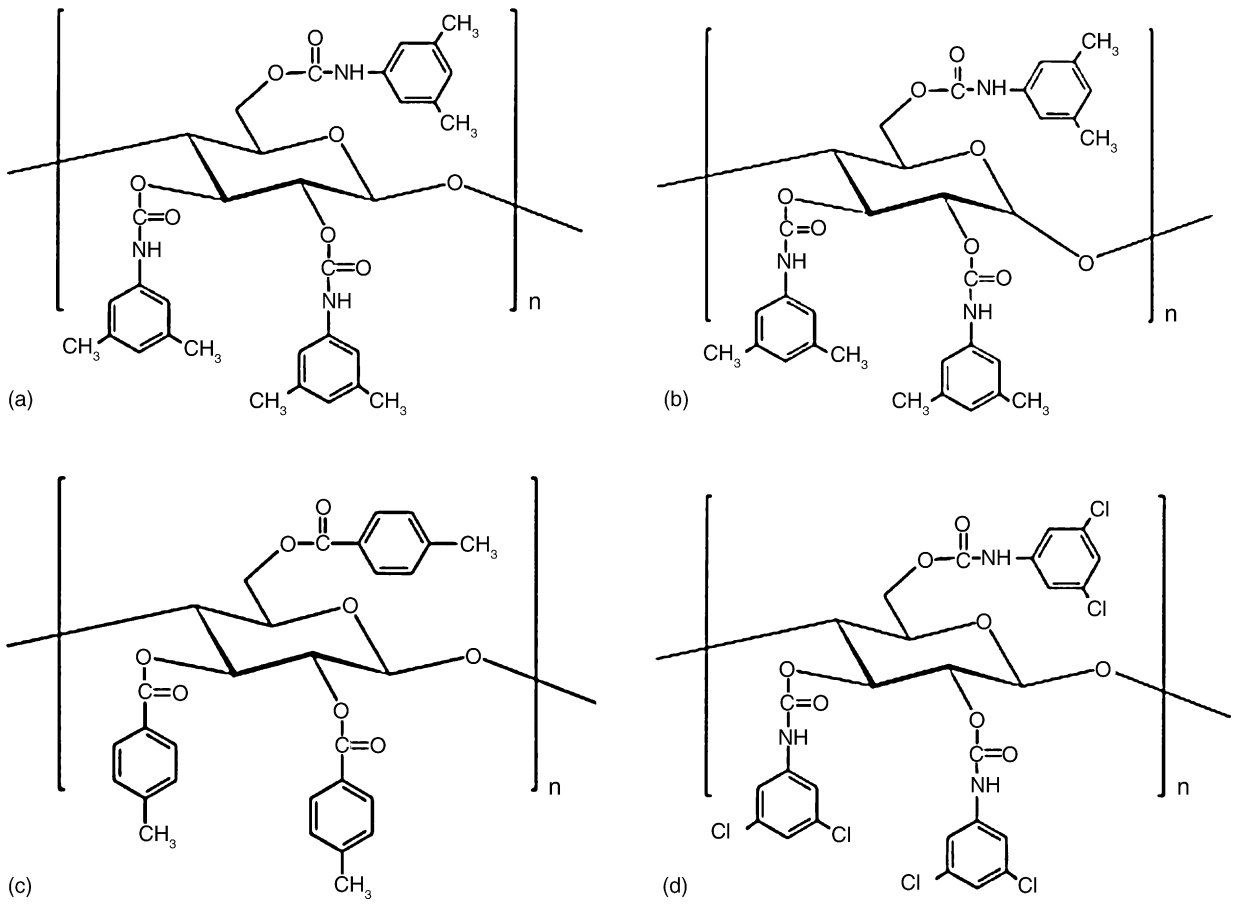

Fig. 4. Structures of the polysaccharide derivatives utilized as selectors in NACEC. Reprinted with permission from ref. [29].

critically depends on the employed protocol for the preparation, all have a profound effect on the enantiomer distinction ability of the CSP. The dipolar carbamate and ester groups, respectively, are located in close proximity to the core of the polymeric strand, and are supposed to drive the intermolecular interaction into cleft-like binding pockets or grooves that are formed by the pending aromatic moieties or by pockets embedded in the ordered supramolecular assemblies. The geometries of the clefts are largely determined by the type of derivative, i.e. carbamate or ester, and the hyperstructure itself, which in turn depends on the employed synthesis protocol and polysaccharide (cellulose or amylose) used as core structure. In addition, the differently substituted aromatic residues possess distinct π–π interaction nature and strength. Hence, it is easily understandable that by such a small number of relatively closely structurally related selectors a very broad spectrum of chiral solutes can be resolved into individual enantiomers. In fact, they are complementary in terms of enantioselectivity and reversal of elution order has been reported upon variation of the derivative as well as a change of the synthesis protocol (that altered the hyperstructure). Although the nonaqueous polar organic mode does actually not represent preferential conditions as mentioned above, its principal applicability for enantioselective NACEC has been demonstrated for a reasonably broad spectrum of chiral solutes, which includes a variety of differently structured chiral drugs (see Table 1). More studies, however, will be necessary to explore the full spectrum of applicability.

It was anticipated by Chankvetadze and Blaschke that for CEC with its specifics and characteristics and in particular its distinct mode of eluent driving force a dedicated CSP design will be demanded, in order to be able to fully exploit its potential and achieve highly efficient separations that are prompted by theory. Along this line, a number of stationary phase parameters needed to be re-evaluated and were optimized systematically. The main results of these studies can be summarized as follows.

(i) *Chemical nature of support*: The same problems regarding EOF generation as discussed above for the poly(diphenyl-2-pyridyl methacrylate) CSP are pertinent for coated polysaccharide CSPs. The coating of the neutral selectors in a dense layer onto wide-pore particles covers the active ionized functional groups and surface charge, and thus exerts a shielding effect which reduces the EOF velocity. Silica and aminopropyl-silica particles, for which the EOF is a bulk property of the net charge of cationic amino groups and anionic residual silanols, have been tested as supports [35]. Both were found to be principally useful for NACEC with

methanolic BGE, as they generated an EOF strong enough even after coating of the selector. It was cathodic for silica and anodic for aminopropyl-silica, as expected. No clear preference, though, could be derived from the comparative study with coated cellulose tris(3,5-dimethylphenylcarbamate). However, overall the aminopropyl-silica seems to be favorable as support with regards to EOF velocities in particular under acidic conditions, as already pointed out above [17], and with regards to avoiding non-specific interactions in case of basic solutes. In fact, in the majority of studies (see Table 1) aminopropyl-silica was utilized as carrier material for the coating. The typical electroosmotic mobility obtained, e.g. with 20% (w/w) Chiralcel OD coated onto aminopropyl-silica and use of 10 mM ammonium acetate in MeOH at various pH* (adjusted by addition of acetic acid), was in the range of -5×10^{-5} cm^2 V^{-1} s^{-1} to -8.5×10^{-5} cm^2 V^{-1} s^{-1}, with the maximum around pH* 5) [29].

(ii) *Selector loading* [29,31–33,55]: The most important factor of the polysaccharide CSPs turned out to be the amount of selector coated onto the surface. It is of central importance for EOF velocity, retention factors, enantioselectivity and efficiencies likewise. The above described shielding of ionizable moieties at the support surface more and more decreased the EOF, the more selector was coated onto the surface. For example, the elution time of the EOF-marker thiourea steadily increased from about 4 min at 5% (w/w) selector loading to 10 min at 20% (w/w) for cellulose tris(3,5-dimethylphenylcarbamate) CSP based on 5 μm 2000 Å silica and 10 mM ammonium acetate as eluent [31]. The thicker coating offers more adsorption places and therefore retention factors increased as expected, while the optimum of separation factors was typically found at 5% (w/w) in this study [31]. On the other hand, striking differences between nonaqueous capillary liquid chromatography (CLC) and CEC regarding the dependencies of efficiencies on selector loading were noticed [31,32]. In nonaqueous CLC, the lower theoretical plate height was typically attained when the selector loading was increased from 2 over 5 to 10% (w/w). The gain of efficiency thereby resulted mainly from flatter Van Deemter plots (*H*/*u* curves) and is indicative for a better mass transfer in the CSPs with a thicker coating. In contrast, in NACEC the CSPs with thinner coatings (5%, w/w or less) revealed higher efficiencies and very flat *H*/*u* curves with the optimum typically at the highest achievable flow rate. For example, theoretical plate heights *H* of less than 5 μm were reported for a CSP with 5% (w/w) selector, i.e. the reduced plate heights reached unity, which is remarkable for enantiomer separation. Hence, according to Chankvetadze et al., to succeed in highly efficient enantiomer separation, it is advised to utilize coated polysaccharide CSPs in the NACEC mode with a coating density as thin as possible. Fast enantiomer separations may be accomplished and very high theoretical plate numbers have been reported, e.g. 177,000 m^{-1} for Troeger's

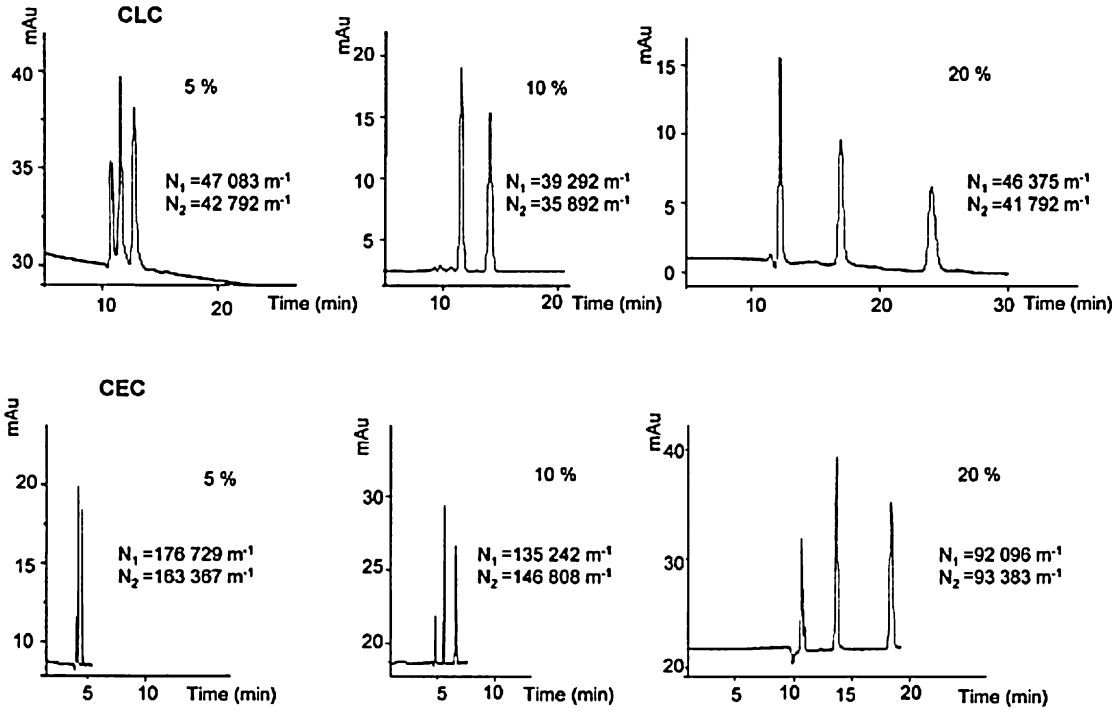

Fig. 5. Enantiomer separation of Troeger's base using cellulose tris(3,5-dimethylphenylcarbamate based CSP: effect of selector loading on the achieved separations. (a) Nonaqueous CLC, and (b) NACEC. Conditions: 5 μm, 2000 Å silica particles coated with 5, 10, and 20% (w/w) of the selector. The 10 mM ammonium acetate in MeOH. Reprinted with permission from ref. [31].

base (Fig. 5). The loading capacity of such a material of course is lower and care has to be taken not to overload the column [33].

(iii) *Pore size* [30,35]: In principle, EOF originates anywhere at the surface of the stationary phase and support, respectively, i.e. also on the intraparticle surface. This may generate intraparticle pore flow that may favorably contribute to the flow characteristics and dynamics in CEC and lead to an enhancement of relative EOF velocities and mass transfer through convection in intraparticle pores. Such a perfusive intraparticle flow, however, may be diminished by excessive double layer overlap which may occur in narrow pores in particular at the low ionic strength BGEs that are normally employed in CEC. Hence, wide pore silica particles were supposed to show better performance in terms of EOF velocities and peak efficiencies. To verify this, comparative experiments with particles differing in the nominal pore diameter in the range between 60 and 2000 Å all coated with 20% (w/w) cellulose tris(3,5-dimethylphenylcarbamate) [30] were carried out. Indeed, electroosmotic mobility was by a factor of about 3 higher on the 1000 Å wide-pore particles than on the 60 Å material, presumably due to the detrimental effect of double layer overlap in the latter material. This was confirmed when the ionic strength of the methanolic BGE was varied using the modified particles with distinct pore diameters [34]. While electroosmotic mobility, as expected, decreased for the wide-pore particles when the ionic strength was increased, it increased for the narrower 120 Å modified silica beads, most probably due to reduction of double layer overlap. The favorable effect of a wider pore diameter on the plate numbers was clearly revealed by very flat *H*/*u* curves of the 1000 and 2000 Å particles conforming with the perception of a favorable mass transfer owing to convective intraparticle flow [30] (Fig. 6). The *H*/*u* curves with 120 Å and in particular 60 Å materials, in contrast, showed a very steep slope indicating a strong resistance to mass transfer. The convective pore flow in NACEC, not available, for example, in CLC, has led to a proportionally higher gain in efficiency with wide-pore particles in NACEC compared to CLC. For example, plate count was by a factor of 1.3 higher in NACEC than CLC with 200 Å pore diameter but even by a factor of 6.5 enhanced with 1000 Å particles [35]. While there was a trend to lower enantioselectivity when the pore diameter was larger [30], resolution was significantly improved due to the gain of chromatographic performance. The loss of enantioselectivity may be attributed to the reduction of active surface area in the wide-pore materials. Overall, the wide-pore materials exhibited better NACEC characteristics and were preferentially used for further investigations.

(iv) *Particle diameter* [30,31]: The particle size dependency of efficiencies followed the expected trend; a gain of plate numbers by a factor of about 2 could be achieved when 5 μm particles (120 Å) were substituted by 3 μm beads (120 Å) [30]. Both favorable effects, small particle diameter (3 μm) and macropores (>500 Å), could unfortunately not be combined due to lack of availability of such silica materials. As the gain of efficiency was proportionally larger with the wide-pore materials and also their flow characteristics was better, 5 μm 1000 Å or 2000 Å silica particles turned out to be the preferred choice as support.

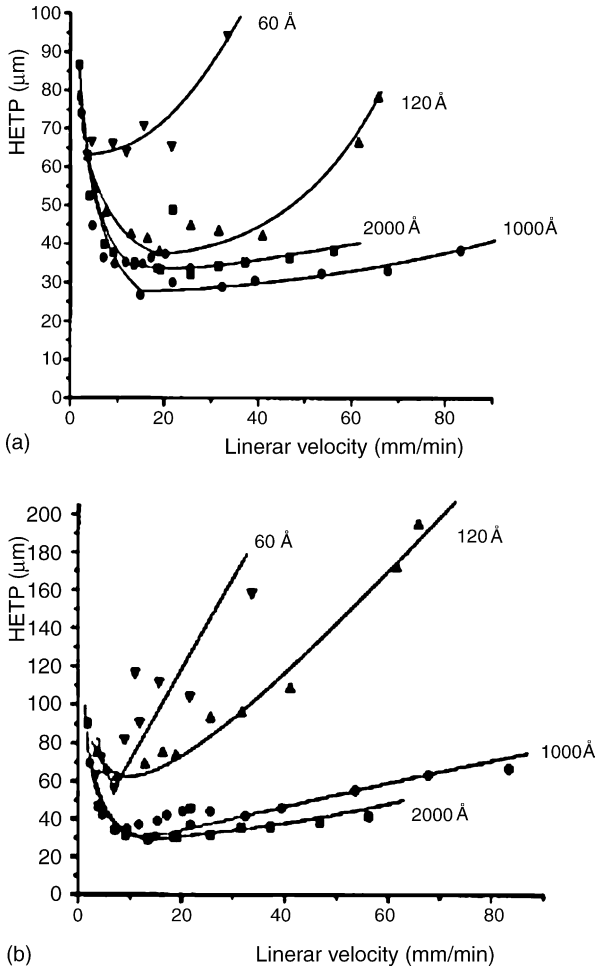

Fig. 6. Van Deemter plots for (a) thiourea (flow marker) and (b) second peak of trans-stilbene oxide using CSPs prepared by coating of cellulose tris(3,5-dimethylphenylcarbamate) (20%, w/w) on silica of varying pore size. Eluent, 2.5 mM ammonium acetate in MeOH (pH* 7.7). Reprinted with permission from ref. [30].

Besides the stationary phase variables also the mobile phase parameters and other experimental conditions have been thoroughly investigated. While Chiralcel OJ showed less suitability in polar organic mode and therefore also in NACEC, Chiralpak AD, Chiralcel OD and in particular the cellulose tris(3,5-dichlorophenylcarbamate) have proven their excellent applicability in the polar organic mode and NACEC. MeOH containing 2–10 mM ammonium acetate appeared to be the standard eluent in the proposed NACEC studies. However, complementary selectivities have

been achieved with distinct solvents or solvent mixtures [29–32,55]. For example, trans-styrene oxide enantiomers were better resolved with EtOH than MeOH on amylose tris(3,5-dimethylphenylcarbamate) based CSP, probably due to strengthened dipole–dipole interactions [29,30]. Metomidate was separated into enantiomers with ACN, while no separation could be achieved with MeOH, maybe owing to detrimental strong competitive hydrogen bonding effect of the latter [32]. On the other hand, if hydrophobic interactions are important for stereodistinction, addition of increasing amounts of water may improve the separation as was found, e.g. for Troeger's base [55].

With both optimized mobile phase conditions and 5 μm 2000 Å silica or aminopropylsilica coated with 5% (w/w) of the polysaccharide selector (or even less) enantiomer separations with up to 400,000 N/m have been afforded. However, such low selector concentrations require a high intrinsic enantiomer recognition ability of the selector, as indicated by the authors [56]. If this cannot be provided, a higher loading of the selector can be envisioned, thereby sacrificing a part of the plate numbers. Overall, the studies by Chankvetadze and co-workers clearly revealed the potential of polysaccharide based CSPs and convincingly illustrated the major influential factors to be optimized in order to achieve highly efficient enantiomer separations by NACEC.

In all these aforementioned studies, the polysaccharide derivatives were immobilized non-covalently by the coating procedure. These CSPs are, of course, restricted to solvents that do not dissolve the polysaccharide derivative. Covalently bonded polysaccharide phases, in contrast, that possess solvent resistance to any of the organic solvents utilized in RP, NP, and PO enantiomer separation modes, thereby having broader application spectrum and providing more flexibility in the design of the enantiomer separations, were prepared by Zou and coworkers [8,36,37] (Fig. 7a). These bonded polysaccharide CSPs were evaluated in NACEC (in NP-like mode with hexane-based eluents containing also alcohols and THF) and pressure-assisted NACEC mode in comparison to the analogous aqueous system. For a variety of solutes, the NP mode with an apolar mobile phase composed of hexane–MeOH–2-PrOH–THF turned out to yield higher enantioselectivity than more polar eluents. For example, the α-value of praziquantel as test compound increased with the increase of percentage of hexane, while concomitantly EOF constantly decreased. It is noted that the use of THF, which was found to have a beneficial effect on the enantioselectivity, resolution and efficiencies in several instances [37], can only be used with the bonded polysaccharide CSPs, but not with the coated analogs, because it dissolves the polysaccharide derivatives. Initially, the cellulose 2,3-O,O-bis(phenylcarbamate) selector was anchored regioselectively at position 6 of the glucose unit to aminopropylsilica (CSP II) leaving a certain portion of the amino groups of the spacer unreacted which were supposed to be the major source for EOF generation. However, the following problem emerged: the residual silanols still present at the surface counteracted

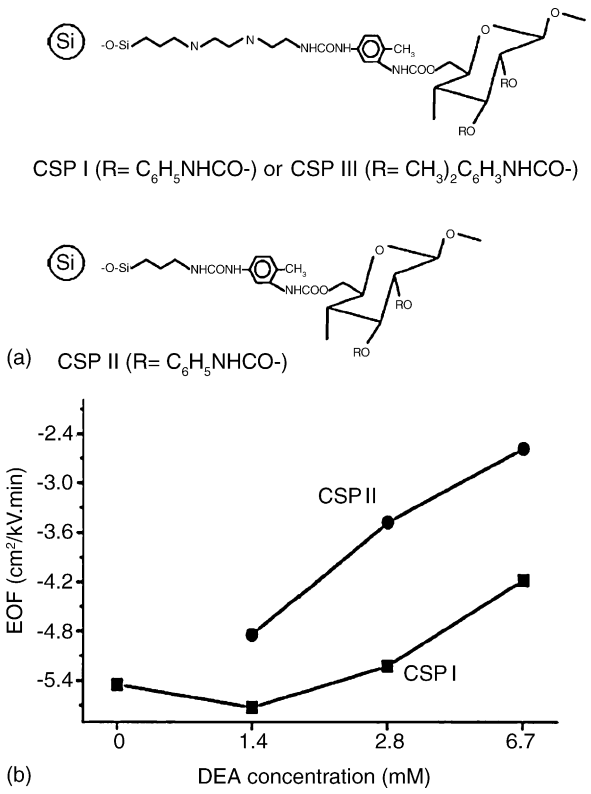

Fig. 7. (a) Structures of investigated bonded cellulose carbamate CSPs, and (b) comparison of EOF behavior of bonded cellulose CSPs based on aminopropylsilica as support and corresponding CSP with positively charged spacer based on diethylenetriaminopropylsilica. (b) Conditions: EtOH containing 14.2 mM acetic acid and various amounts of diethylamine (DEA); voltage, −15 kV. Reprinted with permission from ref. [36].

to a significant extent the EOF force of the amino groups and thus the mobile phase composition was critical in terms of EOF strength and direction. For example, the NP-like nonaqueous eluent composed of hexane–MeOH–2-PrOH–THF (35:50:10:5, v/v) containing 5 mM acetic acid–triethylamine allowed a reversal of EOF to the expected anodic direction, the EOF was cathodic with aqueous ACN–phosphate buffer (60:40, v/v) (2 mM phosphate, pH 6.9) and by a factor of about 20 higher than with the nonaqueous eluent. For the reversal of EOF, the triethylamine was made responsible that presumably deactivated the residual silanols by ion-pairing. However, also with these conditions the EOF was weak. As a consequence, elution times were relatively high with nonaqueous conditions and required to be assisted by pressure, e.g. a pressure of 2 bar applied to the inlet end has led to a reduction of run times by 50%.

In a subsequent study, a doubly positively charged spacer was devised to overcome the problem of poor EOF speed with employed nonpolar conditions [36]. Instead of immobilizing the polysaccharide selector onto aminopropylsilica, diethylenetriaminopropylsilica served as support for the bonding (see Fig. 7a, CSP I). Thereby the nitrogen content of the amino-modified beads could be raised by 50% (according to elemental analysis) and the introduction of the posi-

tively charged spacer, in fact, amplified the EOF (ca. 50% increased but still moderate; ca. -9.5×10^{-5} cm^2 V^{-1} s^{-1} at maximum) (see Fig. 7b). A variety of solutes were separated on both CSPs including Troeger's base and praziquantel, but with higher speed on the CSP with the positively charged spacer. While the aqueous mode provided higher efficiencies, the nonaqueous mode produced higher enantioselectivities in the majority of cases. A seriously disturbing problem, however, appeared in the course of the multiply charged polysaccharide CSP with positively charged spacer: It was reported that it was hard to get good frits on this CSP due to the poor fusion properties of the positively charged particles. Since harsh conditions were obviously required for making the frits, this may have negatively affected the efficiency of the columns. Another analog prepared later by chemically bonding methacryloyl-modified cellulose 3,5-dimethylphenylcarbamate onto methacryloyldiethylenetriaminopropylsilica by copolymerization had broader spectrum of applicability in NACEC mode using short end injection [37].

5.2. Macrocyclic selectors

CSPs based on cyclodextrins (CDs) and macrocyclic antibiotics (vancomycin and teicoplanin) have been examined in NACEC (using polar organic mode). Both type of selectors, cyclodextrins and macrocyclic antibiotics as well, can be classified into intermediate oligomeric and macrocyclic selectors that recognize and bind guest molecules by inclusion complexation into their macrocyclic cavities. While CDs do so by solvophobic interactions as major driving force for complex formation, inclusion is driven by H-bonding, dipole–dipole and/or electrostatic interactions in case of the antibiotic counterparts.

Wistuba et al. prepared packed capillary columns (100 μm i.d.) with 3 μm ChiraDex-beta and 5 μm ChiraDex-gamma (β-CD, γ-CD attached to silica via carbamate linker) [9] and operated these capillary columns by pressure-assisted NACEC with methanolic eluents and MeOH–ACN based mobile phases, respectively, and for the purpose of comparison also with aqueous mobile phases. The nonaqueous eluents contained MES buffer in 5–13.5 mM concentrations, readily soluble in this concentration range. Obviously MES was adsorbed to the surface of the CSP (presumably by interaction with the carbamate group and/or spacer), because anodic flow resulted being favorable for the intended separation of the Dns-amino acid enantiomers. Pressure-assistance stabilized the flow through circumventing the problem of bubble formation (outgassing) at the end frit and accelerated the otherwise slow analysis. With the nonaqueous methanolic conditions it could be taken profit of faster elution times compared to aqueous eluents. While the addition of ACN (30–70%, v/v) to MeOH gradually enhanced the EOF and lowered retention, R_S was impaired dramatically with ACN. On contrary, admixing minor amounts of water had a beneficial effect on enantioselectivities and vastly improved R_S. Overall, high selectivity and fast separation at same time seem to be contradictions in this system and the preference of aqueous conditions reflects the expected behavior that reasonably strong solvophobic interactions are required for effective enantiomer recognition. On contrary, MeOH–ACN eluents switch off such interactions.

The success of the polar organic mode in HPLC enantiomer separation with macrocyclic antibiotic phases evidently prompted the use of such conditions in CEC too and so it is not surprising that several NACEC studies with macrocylic antibiotics CSPs have been performed by different groups in this mode. Vancomycin [38–40], teicoplanin, and teicoplanin aglycone (TAG) based particulate silica-supported chiral stationary phases (Fig. 8), either supplied from commercial sources (Chirobiotic V [39], Chirobiotic T [41,42], Chirobiotic TAG [43]) or home-made materials [20,38,40] have been tested after slurry packing into FS capillary of 50–100 μm diameter, and their behavior was largely consistent with regards to achieved results and expectations from viewpoint of theory and HPLC extrapolations.

Few peculiarities in column technologies deserve to be mentioned at this point. Typically, the silica particles (3.5 or 5 μm with 100 Å pore size) modified with the antibiotics selectors (selector loadings ∼130 μmol/g or 0.36 μmol/m^2 [20]) were slurry packed into the capillaries creating columns with the mentioned duplex nature having a packed and an open segment [39,41–43]. Wikström et al., on contrary, showed that an in situ derivatization procedure of a prepacked capillary column with reactive achiral diol-silica (5 μm) is a viable route to CEC capillary columns too [38,57]. The vancomycin selector was immobilized onto these packed reactive particles after oxidation of the diol moieties to aldehydes by reductive amination. On the other hand, Fanali and co-workers fully packed their capillaries over the entire length into three distinct segments of which only the middle part contained the vancomycin CSP, while the two outer sections were packed with diol-silica each [20,40]. The first short diol-silica segment accommodated the inlet frit and the longer segment of diol-silica at the outlet end of the capillary the end frit as well as the detection window. The vancomycin-CSP in the middle part was packed into a 23 cm long chromatographic bed. The cathodic EOF of the vancomycin CSP originates from the residual silanols, while the vancomycin selector itself that has a pI of ca. 7 exerts a minor opposing effect under acidic conditions. In order to enhance the cathodic EOF, 25% of bare silica was admixed to both vancomycin CSP and diol-silica as well. Detection was carried out through the packing in a position which was devoid of vancomycin. The loss of detection sensitivity due to presence of the diol particles in the detection cell was obviously minimal and supposedly was compensated by less peak broadening, because the migrants did not need to pass an end frit before detection thus omitting this major dispersive factor. This specific design was selected for the following reasons: (i) more stable columns could be obtained and less problems with outgassing were reported. (ii) The frits can be made on diol-silica which had

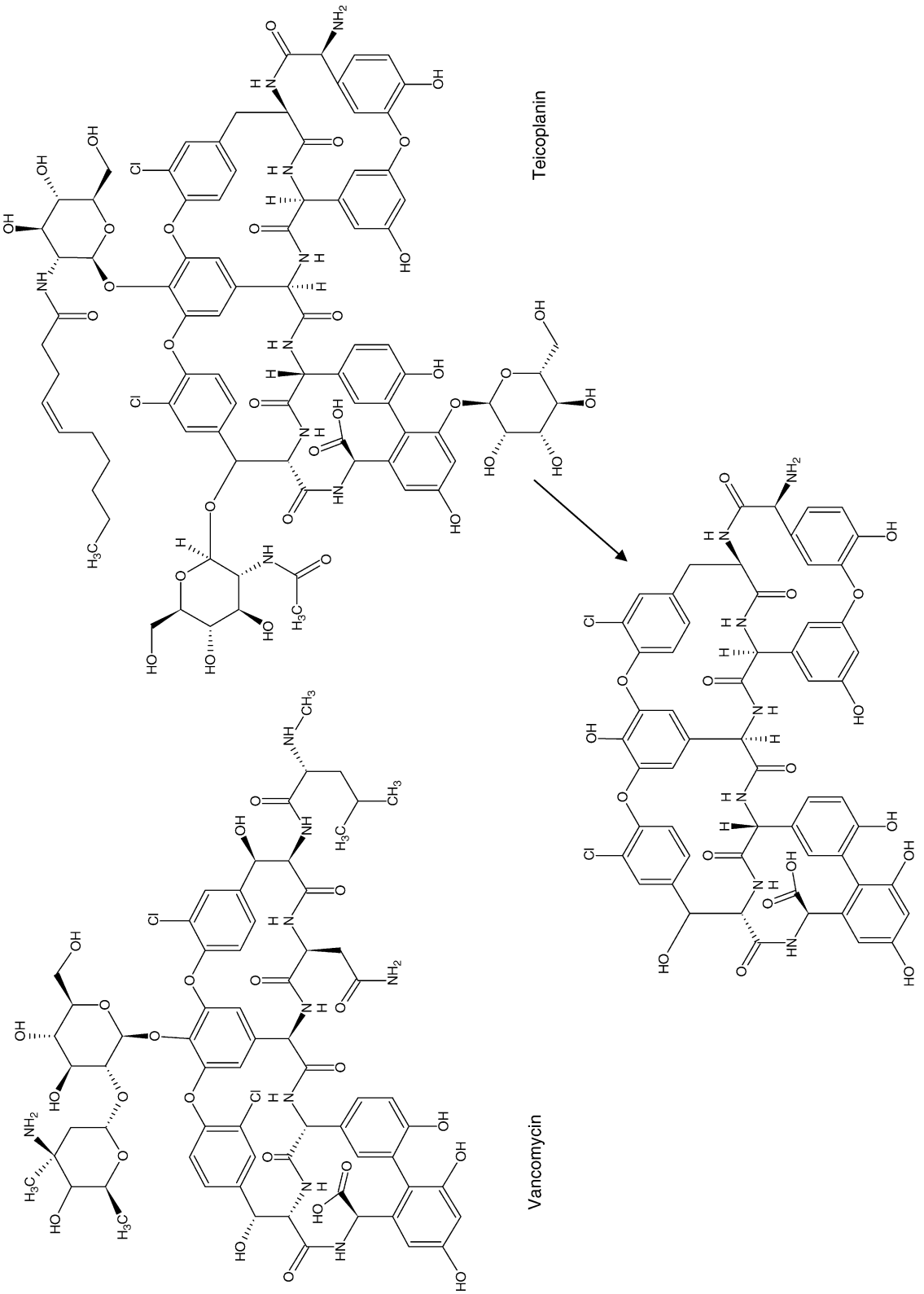

Fig. 8. Structures of macrocyclic antibiotics, vancomycin, teicoplanin and teicoplanin aglycone (TAG), bonded onto silica supports for NACEC use.

better sintering properties than CSPs. (iii) The frit fabrication procedure must be optimized only once and can then be used for different types of packings. Otherwise, the frit is made of the chromatographic packing and optimization of the frit fabrication is required for each packing. In a later study, in which 3.5 and 5 μm particles were comparatively evaluated with the two distinct column designs (duplex nature and fully packed) [20], Fanali and co-workers suggested to return to the common column technology. The admixing of bare silica that generously provides silanols was found to give rise to excessive non-specific interactions with cationic analytes, which has led to low plate counts in particular for the 3.5 μm particles. Efficiencies, in particular of 3.5 μm particles, increased dramatically by a factor of 2–10 without admixing silica. For example, a minimal reduced plate height h_{red} of ∼1.2, which was favorably located at the highest attainable flow rate, could be achieved with the 3.5 μm plain vancomycin column. Elution times were only moderately increased (∼10–20%) when silica was omitted [20].

In addition to these packed capillary column technologies, Kornysova et al. successfully fabricated hydrophilic polyacrylamide type monolithic capillary columns by a post-modification approach. First, monolithic capillaries based on the acrylamide monomers *N*-(hydroxymethyl)acrylamide, *N*,*N*′-piperazine diacrylamide, and vinylsulfonic acid (as ionic monomer admixed to provide permanently ionized functionalities for EOF generation) were copolymerized forming the continuous bed. Subsequently, the monolith was derivatized with vancomycin by above described oxidation/reductive amination reaction scheme. This monolithic column unfortunately did not exhibit any enantiomer recognition abilities in the nonaqueous polar organic mode, contrasting with expectations, but a few racemates could be resolved in the RP mode [58].

While the RP mode turned out to be preferable in this particular case of polyacrylamide monolith as well as in a later performed study on the stereoisomer separation of amino acids and peptides on Chirobiotic TAG [59,60], the other CEC studies with macrocylic antibiotics CSPs reported uniformly on a more enantioselective nonaqueous polar organic mode compared to the hydroorganic RP mode which holds in particular for the separation of chiral bases on vancomycin and TAG [38–40,43]. Vancomycin CSP separated in NACEC mode thalidomide (Fig. 9), β-blockers and β-sympathomimetics like terbutaline [57] and in addition some other basic drugs [40], while no basic compounds could be resolved in hydroorganic RP mode [39]. Complementary CEC enantiorecognition capabilities of the two distinct mobile phase modes were reported for the teicoplanin CSP [41]. For example, β-blockers were not resolved in reversed-phase, but in polar organic mode only. However, in RP mode also a few neutral and acidic SAs could be resolved into enantiomers. The new Chirobiotic TAG CSP, which has the sugar moiety of teicoplanin cleaved, has shown to possess significantly different enantiorecognition behavior compared to the parent glycopeptide CSP. This has been confirmed by NACEC as

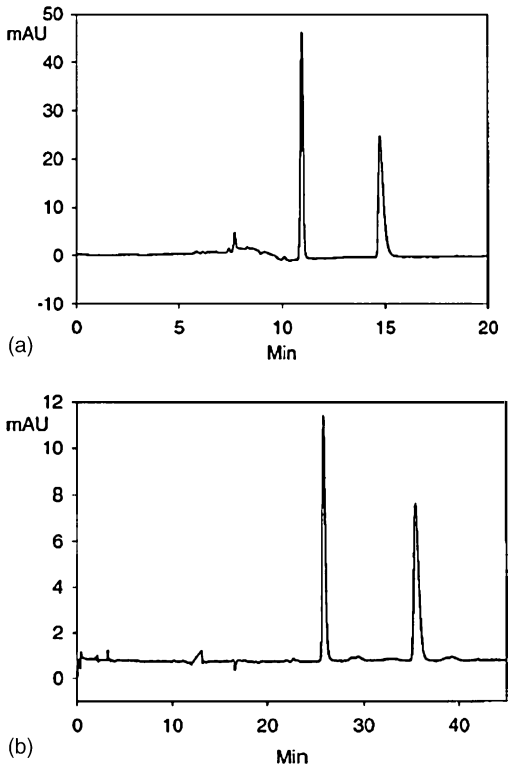

Fig. 9. Comparison of CEC enantiomer separations of thalidomide on vancomycin CSP and polar organic (a) as well as hydro–organic reversed-phase mode (b). Conditions: (a) MeOH–ACN–TEA–AcOH (80:20:0.1:0.1, v/v); voltage, 20 kV; *T*, 15 °C. (b) Eluent, ACN–0.1% triethylammonium acetate buffer (pH 4) (30:70, v/v); voltage, 25 kV; *T*, 15 °C. Reprinted with permission from ref. [39].

well [43]. In the polar organic mode, however, it had similar spectrum of application as the parent teicoplanin CSP, which was mainly comprised of chiral drugs with amino alcohol structures. In contrast, for the separation of free amino acids that could not be resolved into enantiomers on teicoplanin aqueous conditions were required. Because of the slow EOF under these conditions the additional pressure application of 1.2 MPa which was possible with the internal pressure system of the employed CEC system helped to slightly accelerate the analysis and had only a moderately negative effect on R_S.

As a common trend, regardless of type of antibiotics selector, the polar organic mode worked better in NACEC with a low percentage of acetonitrile (typically in the range between 5 and 40%, v/v). Such eluents tended to outperform conditions with lower and in particular higher ACN content. Although a high ACN percentage could yield due to the more favorable ε/η ratio faster electroosmotic flow, the optimum in terms of R_S was typically observed with high MeOH content (at least 60%, v/v). This fact was explained by a reduction of non-stereoselective interactions through competitive H-bonding stemming from non-specific adsorption of cationic solutes to acidic silanols, the existence of which has been inferred from tailing peaks observed despite triethylamine in the mobile phase [39,57]. Typical plate counts achieved in the different studies can be derived from Table 1. Fanali et al.

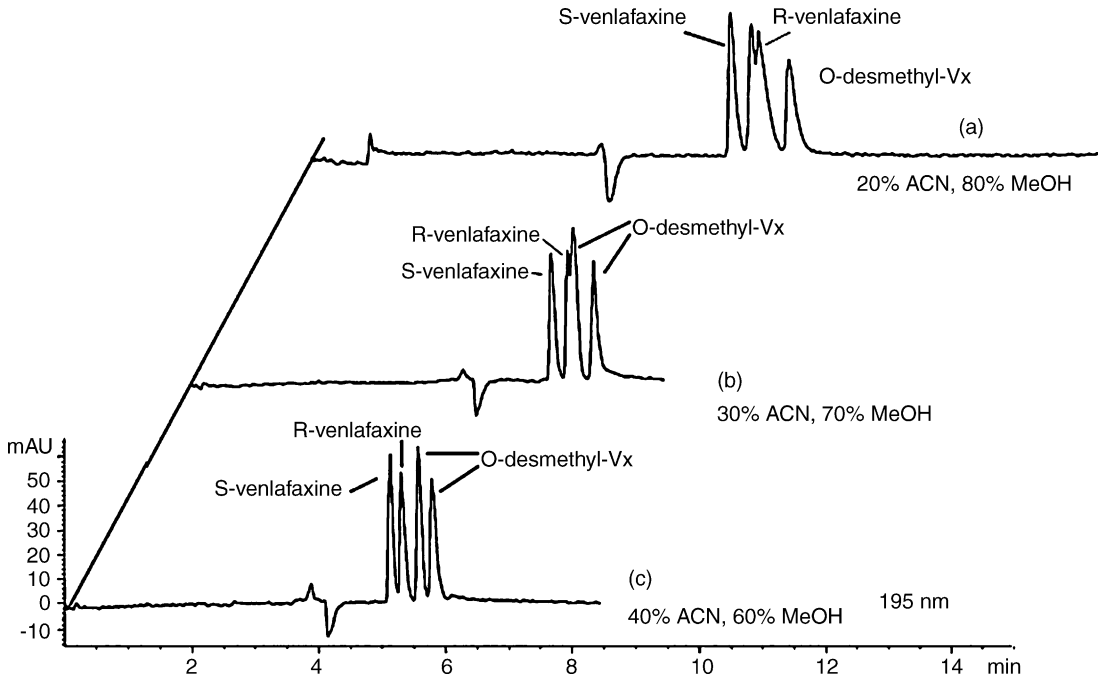

Fig. 10. Electrochromatograms of the simultaneous separation of venlafaxine and its metabolite (O-de–methyl–venlafaxine) on vancomycin-based CSP using different ACN–MeOH ratios (13 mM ammonium acetate as electrolyte; applied voltage, 30 kV). Reprinted with permission from ref. [40].

[40] thoroughly investigated solvent effects and found 40% (v/v) ACN as a good compromise yielding satisfactory resolution in short elution times for a wide variety of solutes. In one example, venlafaxine and its O-desmethyl metabolite could be baseline separated into enantiomers simultaneously (see Fig. 10), and ACN affected both the chiral and achiral selectivity. The substitution of MeOH by other alcohols, viz. EtOH, 1-PrOH, and 2-PrOH had a deleterious effect on R_S, which decreased in this order, and likewise on EOF.

The principal practical applicability of NACEC with teicoplanin based CSP and its suitability for enantiomeric excess determination in a pharmaceutical quality control laboratory was demonstrated by Carlsson et al. [42]. The NACEC separation of metoprolol was fully validated to assess the overall performance and suitability for the enantiomeric purity determination of metoprolol enantiomers. Separations in the polar organic mode with 5% (v/v) ACN in MeOH yielded R_S of 2.5 for metoprolol enantiomers, which was regarded to be sufficient for analysis under overload conditions that may lead to partial R_S loss. Repeatability was tested to be less than 5% R.S.D. for retention times, resolution, and peak area and less than 10% for the plate numbers. Linearity could be proven over the concentration range of 0.125–3.0 mg/mL ($r^2 > 0.995$) as well as at the lower 0.1–3% levels related to the main enantiomer ($r^2 > 0.985$) (the latter series of experiments was envisaged to substitute analysis of samples spiked with minor enantiomer at the 0.1–1% level for validation of sensitivity, because available standards of both (S)- as well as (R)-metoprolol contained considerable amounts of enantiomeric impurity). LOD and LOQ were as low as 0.09 and 0.03 area% related to the main peak (corresponding to absolute concentrations between 1.35 and 0.45 μg/mL). Spiked samples with known amounts of enantiomeric impurity yielded accuracies of 100.4%. Robustness of the method was assessed by use of an experimental design and also found to be satisfactory. The results of the validation study were judged to conform well with demands for application to the enantiomeric impurity determination. The major limitation was regarded to be the limited capillary column stability and longevity. Another problem mentioned could arise from the lack of commercial CEC capillary columns, an important concern for a pharmaceutical routine laboratory.

5.3. Low-molecular-mass chiral ion exchangers

Bonded silica gel phases have been shown to exhibit a poor EOF characteristics (see above). Owing to derivatization of a significant portion of the silanols of silica beads in the course of covalently bonding the stationary phase to the surface of the silica beads, the residual silanol density after efficient derivatization is low. Since this translates into a weak EOF, such phases are not optimally designed for CEC. The same was even found (as outlined above) for coated CSPs. For this reason, ion exchangers and in particular permanently ionized mixed-mode ion exchangers, which provide high ζ-potentials and strong EOF, have become the stationary phases of first choice in CEC.

To realize such a concept in a similar manner for CEC enantiomer separation we suggested the use of low-molecular-mass chiral anion exchangers (Fig. 11) that have previously been very successful in HPLC enantiomer separation of oppositely ionized chiral compounds. The general

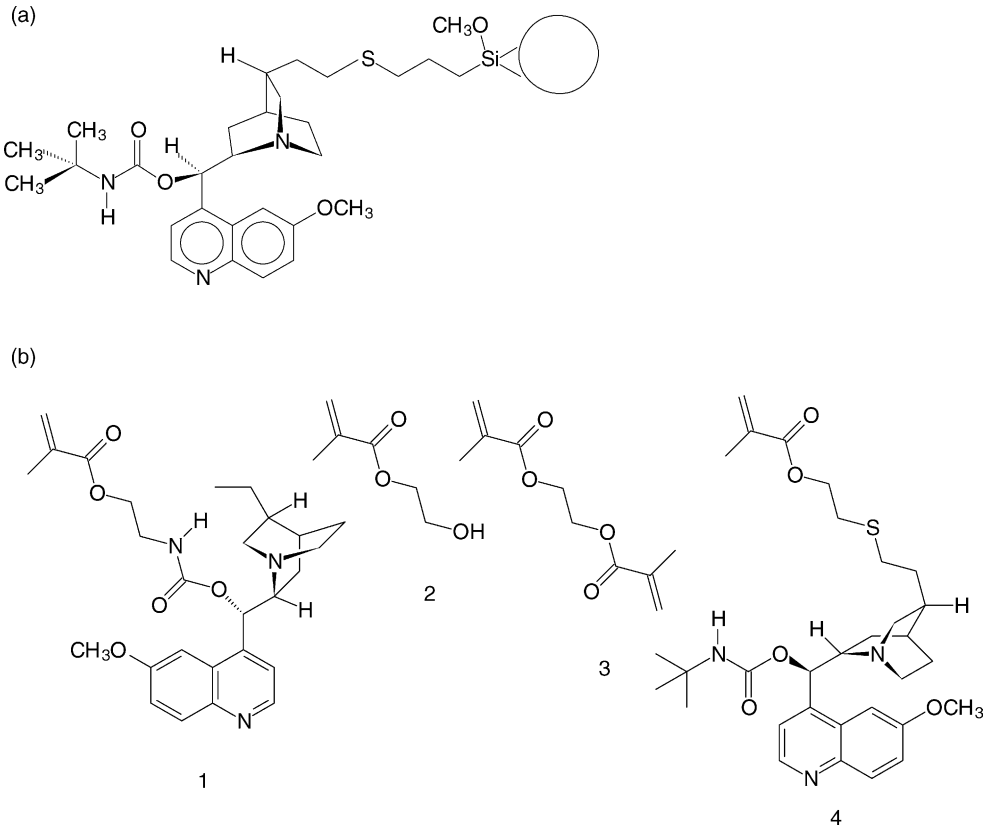

Fig. 11. Structures of chiral ion exchangers used in NACEC: (a) chiral anion-exchanger based on silica particles, and (b) chiral monomers, comonomer and crosslinker used for the preparation of chiral anion-exchange type monolithic CSPs.

characteristics of these CSPs can be summarized as follows: (i) low molecular chiral selectors that carry ionizable groups are immobilized on a chromatographic support (in case of the beaded support 3.5 μm 100 Å silica particles) and due to the relatively small size and surface extension of the selector it can be grafted in a high concentration onto the surface amounting typically to 0.2–0.4 mmol/g silica. (ii) The ionic site of the selector fulfills a double role; it represents the primary ionic interaction site of the selector driving the solute–selector association by a strong ion-pairing mechanism and it is also the main determinant of the ζ-potential and the electroosmotic behavior due to the high selector concentration (the net charge is only to a minor extent influenced by the residual silanols). Since the ionic groups are fully accessible at the surface, a strong EOF with appropriate direction for a faster co-directional separation process is afforded (note: the electrophoretic mobility contribution of the oppositely ionized solutes to overall solute transport needs to be considered). (iii) While ion exchangers in CEC are often operated in the non-interactive mode, i.e. taking advantage of repulsive electrostatic interactions, in the present approach attractive ionic interactions are established in an ion-pairing mode. A strong interaction of the oppositely ionized solutes under hydroorganic conditions with a low ionic strength buffer, typically used in CEC to minimize current generation and avoid the risk of bubble formation, together with other strong π–π interaction, hydrogen bonding and hydrophobic interactions makes it difficult to elute the ionic solutes within reasonable run time in the aqueous CEC mode (see Fig. 12a). The increase of counter-ion concentration, to reduce the actual potential of the ion-exchanger and its ion-exchange capacity, experiences a natural limitation through the current generation and Joule heating of the system. Moreover, the EOF would be reduced at the same time. (iv) Nonaqueous conditions on the other hand allowed to solve this complication: The lower currents in NACEC tolerated the use of higher concentrations of effective counter-ions, which are actually competitive ion-pairing species, and in addition, hydrophobic interactions are weakened too. As a result, the elution times are reasonably fast (see Fig. 12b). As already pointed out above, nonaqueous conditions have been also favorable in terms of system stability (compare baseline stabilities in the both modes in Fig. 12a and b).

Chiral anion exchangers, which conceptionally have the class of chiral acids including various N-derivatives of amino acids and chiral acidic drugs as application spectrum (see Table 1), were investigated in NACEC both as particulate [10,44] and monolithic columns [45–48].

The ζ-potential and EOF characteristics of the silica-based chiral anion exchangers turned out to be a complicated matter under aqueous conditions [61]. Residual silanols and quinuclidinium moieties are counter-acting each other and

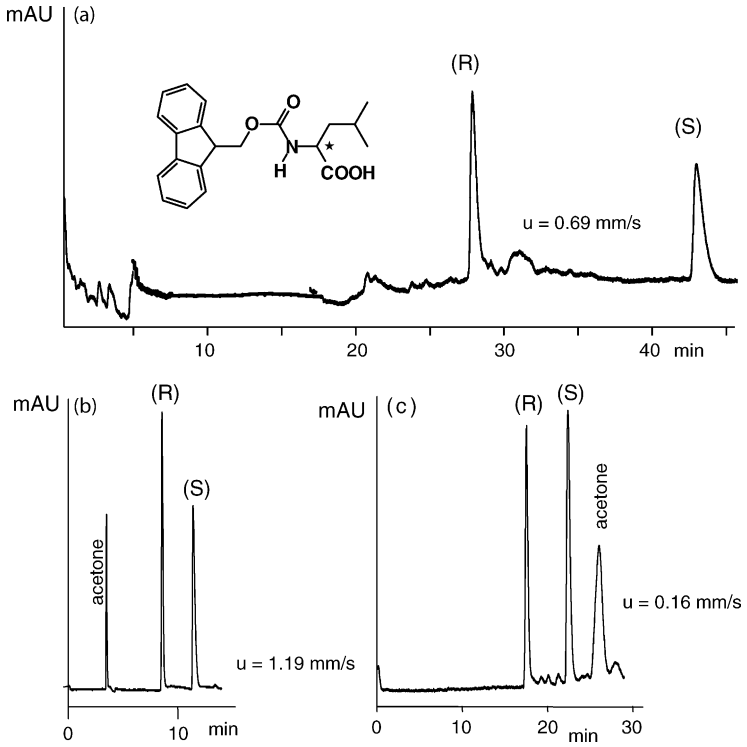

Fig. 12. Enantiomer separation of FMOC-Leu on particulate chiral anion-exchanger: hydroorganic (a) vs. non-aqueous mode (b and c). (b) $\mu_{eo} > \mu_{ep}$, and (c) $\mu_{eo} < \mu_{ep}$. Conditions: CSP: tBuCQN-TPS (Hypersil 120-3 μm); capillary dimension: 0.1 mm i.d., L_{packed} = 25 cm, L_{total} = 33.5 cm, $L_{effective}$ = 25 cm. Mobile phases: (a) acetonitrile: 0.1 mol/L MES (80:20, v/v), pH_a 6.2 (adjusted with triethylamine). *T*, 20 °C; voltage, −25 kV (9.6 μA). (b) 0.2 mol/L acetic acid and 4 mmol/L triethylamine in acetonitrile–methanol (80:20, v/v); *T*, 20 °C; voltage, −25 kV (3.6 μA). (c) Same conditions as in (b), but 10 mmol/L triethylamine. Reprinted with permission in modified form from ref. [10].

the EOF turned cathodic at about pH > 6. In NACEC with ACN–MeOH based eluents containing acetic acid and triethylamine the EOF remained anodic over the entire pH^* range investigated, which is a favorable property and extends the more suitable pH^* range [10]. While the acidic pH^* with excess of acetic acid (e.g. 100-fold molar excess) (Fig. 12b) provided a strong EOF, e.g. -1.7×10^{-4} cm^2 V^{-1} s^{-1} even with a high counter-ion concentration, the superimposed electrophoretic migration becomes more and more important as the acid-excess is reduced and eventually allowed migration of the anionic solute, e.g. FMOC-Leu before the EOF which was weak at such conditions (e.g. 10-fold molar excess of acetic acid compared to triethylamine) (Fig. 12c) [10]. The exceptional enantioselectivity in this system, in which the transport was electrophoretically controlled, was still conserved so that both enantiomers of FMOC-Leu were separated with R_S of about 8.

Some peculiarities, which are typical for this chiral ion-exchange CEC system, emerged in the course of studies regarding the effect of the electrolyte and counter-ion concentration, respectively. In accordance with the ion-exchange mechanism, the retention could be cut down by an increase of the counter-ion concentration (e.g. from 100 to 600 mM) through a stronger competitive or shielding effect exerted by the acetic acid [10]. Thereby, the effective potential of the ion-exchanger and thus the actual ion-exchange capacity were reduced. Although the decreased ζ-potential with such high counter-ion concentrations diminished the EOF substantially, the solute enantiomers eluted much faster at essentially identical enantioselectivity, and the currents were still tolerable. Favorably, the peak tailing disappeared at higher counter-ion concentrations, and a nice symmetrical peak shape with much higher efficiencies could be obtained [10]. Even at a 600 mM counter-ion concentration the EOF marker eluted within 4.5 min on the 25 cm long column.

An ACN content between 60 and 80% (v/v) in the ACN–MeOH eluent was found to represent the optimum for most analytes, and surprisingly the fastest EOF was attained with the eluent containing 40% MeOH in ACN [10].

To corroborate the practical applicability and demonstrate the sufficient stability of the packed NACEC approach, the above described particulate chiral anion exchanger was utilized for the determination of the rotational energy barrier of the reversible enantiomerization reaction of an atropisomeric biphenyl derivative, 2′-dodecyloxy-6-nitrobiphenyl-2-carboxylic acid [44]. To do so, the interconversion kinetics of atropisomeric biphenyl carboxylic acid enantiomers in presence of the anion-exchange type quinine carbamate CSP was studied by a stopped-flow NACEC methodology. After initial separation of the enantiomers in the first part of the CEC column at low temperature, to avoid enantiomerization and peak coalescence of the second kind (plateau-formation

between separated enantiomers due to on-column interconversion), the flow was stopped and the enantiomers of the stereolabile atropisomeric solute allowed to convert, due to their fairly low interconversion barrier, to the opposite enantiomer, i.e. they were allowed to reversibly enantiomerize on-column at a controlled temperature. Then, the voltage and EOF was switched on again. After finishing the separation, an electrochromatogram with a four-peak pattern representing the two original enantiomer peaks and in-between the well-resolved new enantiomer pair formed by the enantiomerization reaction. The conversion could be determined from the corresponding enantiomeric ratios. From conversion at variable enantiomerization times kinetic rate constants could be calculated, which in turn provided apparent activation energies of enantiomerization of 92.9 and 94.1 kJ mol^{-1} for (−) and (+)-enantiomers using the Eyring equation. On the macroscopic level, such different energy barriers for the both enantiomers in presence of the CSP resulted in deracemization, which would approximate a level of 16% enantiomeric excess (ee) after infinite enantiomerization time. The high efficiency of the NACEC method facilitated the complete resolution of the four-peak chromatogram as well as the accurate integration of the minor peaks.

Although the enantioselective anion-exchange NACEC could be designed with appealing chromatographic properties, several problems described in the literature mostly related to frit fabrication, stability and longevity of the packed capillary columns could not be overcome completely. Monolithic columns with the chiral anion-exchange type selectors incorporated into the polymer matrix obtained through in situ copolymerization process of a chiral monomer (in situ approach) [45–48] or attached to the surface of a reactive monolith in a subsequent derivatization (post-modification strategy) [49], both turned out to be viable routes to enantioselective macroporous monolithic columns devoid of the above mentioned limitations.

For the in situ approach, quinidine carbamate was modified with polymerizable methacrylate group to obtain chiral monomer **1**, O-[2-(methacryloyloxy)ethylcarbamoyl]-10,11-dihydroquinidine (Fig. 11b). This chiral monomer was in situ copolymerized with 2-hydroxyethyl methacrylate as comonomer **2** and ethylene dimethacrylate as crosslinker **3** in presence of porogens (cyclohexanol and dodecanol) within untreated fused silica capillaries. Initiation of the polymerization by either thermal treatment or UV irradition yielded different polymer morphologies, even though starting from the same reaction mixture, a fact that added to the complexity, but also flexibility of the monolith preparation. Through systematic studies of the most important stationary phase parameters of the macroporous monoliths such as polymer composition (percentage of chiral monomer, co-monomer type and content, degree of crosslinking) and pore size accompanied by their thorough characterization of physical properties (pore size distributions, surface area), chemical composition (elemental analysis) and chromatographic performance (enantioselectivity tests for test compounds by NACEC and *H*/*u* curves), design considerations could be derived which eventually provided enantioselective anion-exchange type monolithic capillaries for highly efficient enantiomer separations as demonstrated for a number of acidic test compounds (see Table 1).

The monolith performance was found to be governed mainly by the following dependencies [45]: (i) with chiral monomer of about 20% (w/w) (related to total monomers) optimal enantiomer separation factors were reached for most tested analytes. While higher amounts just added retention, lower percentages typically led to both loss of enantioselectivity and efficiency as well. (ii) Of utmost importance turned out to be the type of co-monomer. A more hydrophilic surface adjusted through the polar HEMA comonomer, i.e. its pending 2-hydroxyethyl-moieties had clearly a beneficial effect. In contrast, when the more lipophilic glycidylmethacrylate (GMA) was used as co-monomer, it seemed that non-specific interactions adversely affected the high intrinsic enantioselectivity of the chiral monomer [4] as well as deteriorated the peak performance through a mismatched adsorption/desorption kinetics on the enantioselective and non-enantioselective sites [62]. The study essentially confirmed the earlier findings of Peters et al. [63]. (iii) The crosslinking degree of the chiral monolithic materials was found to be crucial for the flow properties and the dynamics of the electrochromatographic separations. Upon decreasing the EDMA amount and thus the crosslinking degree from 40 to 20% and 10% (w/w) (related to total monomers) the chromatographic efficiency of the monolithic columns could be dramatically improved. Both the maldistribution of the flow (A-term) as well as the resistance to mass transfer were significantly reduced with the lower crosslinking as revealed by Van Deemter curves on three corresponding monoliths that differed in crosslinking and had all a comparable pore size adjusted to 1.1 μm (dry state) by the cyclohexanol–dodecanol ratio used as porogens. Concomitantly the acquirable maximal EOF velocities dropped, e.g. under given conditions, from 1.7 mm/s (40%, w/w EDMA) to 1.2 mm/s (20%, w/w) to 0.6 mm/s (10%, w/w). This trade-off in terms of EOF speed, indicates that the 20% (w/w) crosslinking may be accepted as fair compromise between fast flow and high efficiency. The findings in terms of loss of EOF velocity were attributed to a swelling effect. The swelling is promoted by the less crosslinked materials and reduced thereby the available pore space. Thus the actual pore diameter was assumed to be significantly smaller than measured with mercury porosimetry in the dry state. This would readily explain the loss of EOF velocity, since it has been figured out that with organic polymer monolith columns the EOF velocity is lower the smaller the macropore diameter of the polymer (see above) [46]. Overall, by the swelling a more homogeneous gel-type monolithic bed seemed to be generated which showed the described desirable effects on efficiencies. (iv) Favorably, the less crosslinked monoliths appeared to ‘re-adjust’ in the liquid environment through swelling their pore diameter to the optimal pore size, which was previ-

ously found for a 40% (w/w) crosslinked analog to be around 0.5 μm.

Also the mobile phase parameters and external variables such as temperature were of prime importance. A few peculiarities found during these studies are emphasized at this place: (i) the degree of swelling of the polar polymer chains will depend on the polarity of the employed medium, and is expected to be higher for MeOH than ACN. It is therefore not surprising that the dependency of the MeOH content in ACN on the EOF rate depicted a different relationship with low crosslinked monoliths [47] compared to aforementioned rigid packed column analogs [10]. In fact, with the monolithic column the linear flow velocity steadily decreased when the MeOH content in the eluent was increased, while with the packed column the highest flow was afforded with 40% (v/v) MeOH. Although hard to compare due to completely different morphologies and selector densities in the two type of columns, it is a striking indication for the stronger swelling effect in the MeOH-rich eluents as compared to ACN-rich mobile phases. (ii) A column temperature of 50 °C turned out to be the optimum with regards to accomplished resolution values. This is uncommon, because with packed column analogs it was usually observed in the intermediate temperature range, e.g. around 20–25 °C, as result of two opposing factors, namely decrease of α-values (due to enthalpic control of chiral recognition) and increasing plate numbers (due to enhanced diffusivities) with increasing temperature.

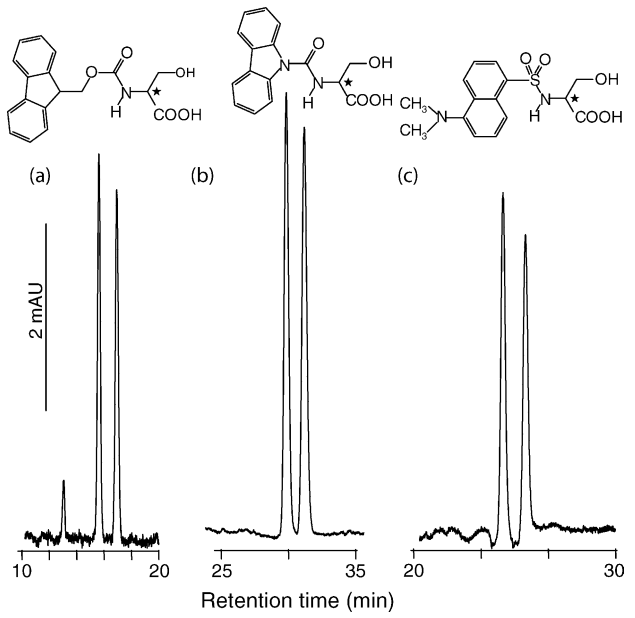

Fig. 13. NACEC enantiomer separations of serine derivatized with different fluorogenic reagents. Monolithic column: polymerization mixture, chiral monomer **4** (Fig. 11b) 8% (w/w), HEMA 28% (w/w), EDMA 4% (w/w), cyclohexanol 15% (w/w), and 1-dodecanol 45% (w/w). UV initiated polymerization 16 h at room temperature. Capillary dimension, L_{total} = 45 cm, $L_{monolith}$ = 20 cm, $L_{effective}$ UV = 36.5 cm, 0.1 mm i.d. Eluent, ACN–MeOH (80:20, v/v) containing 0.4 mol/L acetic acid and 4 mmol/L triethylamine; applied voltage, −25 kV; T, 50 °C. Reprinted with permission from ref. [48].

Enantioselectivities similar or close to those obtained with silica based chiral anion exchanger columns could be obtained on the optimized monoliths for various chiral acids including N-derivatized amino acids. Efficiencies in many instances clearly exceeded those of the packed columns and 250,000 theoretical plates/m could be reached, e.g. for the separation of valine enantiomers derivatized with Sanger's reagent [46]. Short monoliths of only 8.5 cm length allowed fast enantiomer separations in less than 10 min using the short end injection technique [46,47]. Other advantages of the proposed monoliths include the fritless design, because the monolith can be anchored to capillary wall by copolymerization with vinylized FS surface. Opposed to the manufacture of the packed columns, the preparation of such monolithic capillaries, once optimized, is technically simple and a number of capillaries can be easily synthesized in parallel.

Later, a modified cinchonan carbamate type chiral monomer **4**, O-9-(*tert*-butylcarbamoyl)-11-[2-(methacryloyloxy)ethylthio]-10,11-dihydroquinine (Fig. 11b), with a bulky *tert*-butyl adjacent to the carbamate and the methacrylate introduced via the quinuclidine moiety, remote from the active chiral recognition site around the central C9

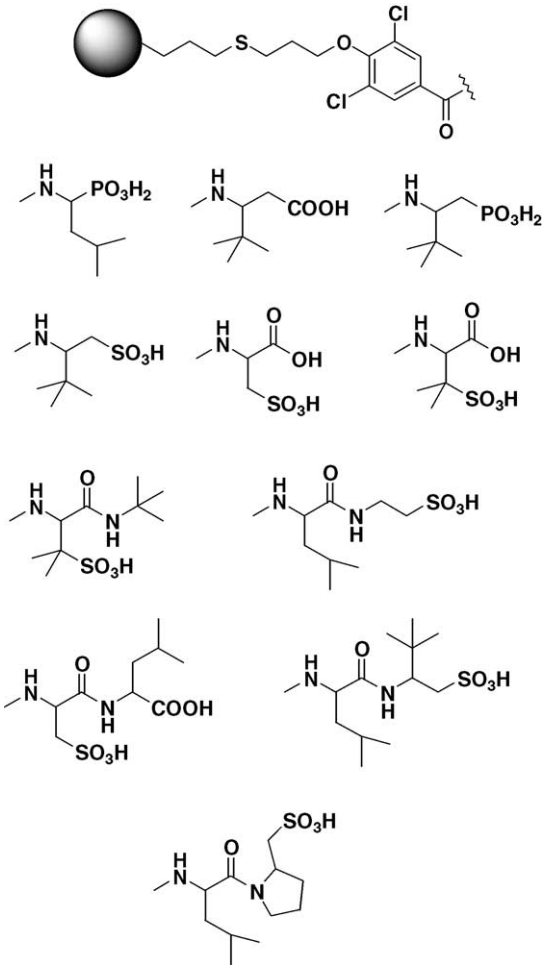

Fig. 14. Structures of investigated chiral cation-exchange CSPs.

stereogenic center, was proposed [48]. The above findings in terms of the optimal design of the cinchonan carbamate functionalized monoliths were confirmed also in this study. Knowledge gained by the earlier work allowed to fabricate optimized monoliths with a minimal number of experiments. The new enantioselective anion-exchange type monolithic columns showed enhanced enantioselectivity, due to the bulky *tert*-butyl group which acts as a steric barrier, and a faster EOF. Representative electrochromatograms are depicted in Fig. 13.

The above described anion-exchange NACEC methods were conceptionally designed to separate the enantiomers of chiral acids. Since only a relatively low percentage, far less than 50% of all racemates that are of importance for pharmaceutical industry, are chiral acidic compounds, the corresponding chiral cation exchangers were developed to complement the spectrum of resolvable racemates and extend the scope of applicability of the enantioselective ion-exchange concept to chiral bases as well.

A variety of new cation-exchange CSPs (see Fig. 14) have been devised utilizing the reciprocity principle of chiral recognition [50]. All the cation-exchange type selectors were constructed of a chiral amino acid, aminosulfonic acid, or aminophosphonic acid synthon that was acylated by a linker acid (4-allyloxy-3,5-dichlorobenzoic acid) with a terminating double bond for immobilization onto thiolpropylsilica (3.5 μm, 100 Å) particles by radical addition reaction. The selectors favorably contain multiple binding sites including besides the primary ionic interaction site, hydrogen donor–acceptor groups, the aromatic π–π interaction site, and steric or van der Waals interaction sites. Through the introduction of the allyloxy group, the π-acidity of the linker acid (which can be characterized by the *e* withdrawing effect of the substituents using the Hammett constant σ which is −0.49) becomes significantly lower than, e.g. of the corresponding 3,5-dichlorobenzoic acid ($\sigma = -0.74$) or 3,5-dinitrobenzoic acid ($\sigma = -1.42$). Nevertheless, it possesses still π–π binding propensity with complementary sites of the analytes which are in case of chiral bases more often π-basic than π-acidic. The dichloro substitution instead of nitro groups was chosen due to its distinct advantage of a cleaner radical addition reaction, while nitro groups are known to be incompatible with radicals and were assumed to yield side products in the course of the immobilization reaction.

It was expected that the strong SCX type materials would be preferred in terms of EOF characteristics, as they were supposed to provide a strong EOF over a wider pH* range. Profound comparative data on the EOF generating behavior of carboxylic, sulfonic, and phosphonic acid materials in non-aqueous electrolyte solutions were, however, not available. Therefore, three analogs varying solely in the acid functionality, i.e. carrying either a carboxylic acid, sulfonic acid, or phosphonic acid (with similar selector loadings between 0.21 and 0.25 mmol/g) were compared with respect to their EOF behavior in NACEC (Fig. 15a) [51]. The pK_a values of the three analogs of Fig. 15a in aqueous solution have been calculated with ACD software to be 4.24 for the carboxylic acid, 1.34 for the sulfonic acid, and 2.12 and 7.69 for the phosphonic acid. According to distinct dissociation constants a different surface charge and ζ-potential and thus electroosmotic

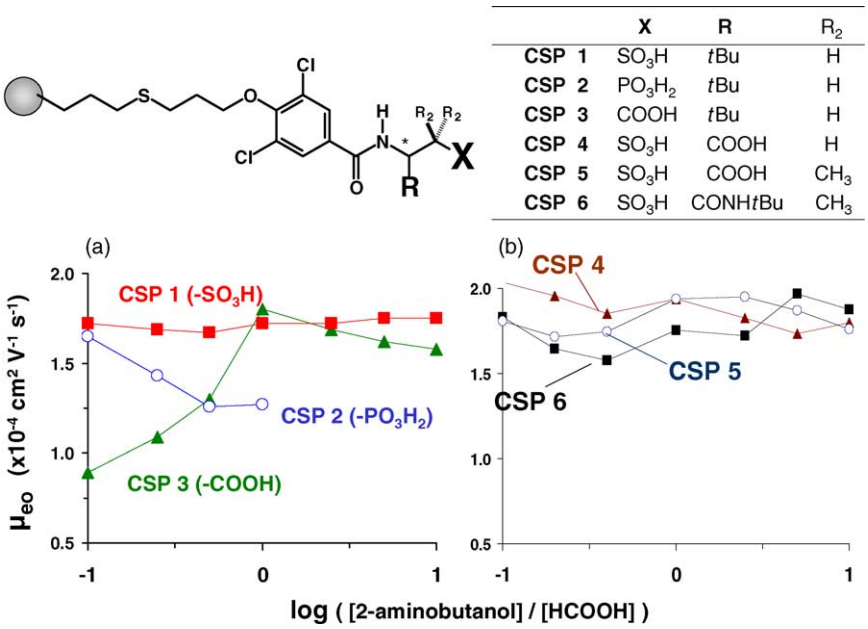

	X	R	R_2
CSP 1	SO_3H	*t*Bu	H
CSP 2	PO_3H_2	*t*Bu	H
CSP 3	COOH	*t*Bu	H
CSP 4	SO_3H	COOH	H
CSP 5	SO_3H	COOH	CH_3
CSP 6	SO_3H	CONH*t*Bu	CH_3

Fig. 15. Dependence of electroosmotic mobility on the base-to-acid ratio: pH* profiles of different chiral cation exchangers. Experimental conditions: base-to-acid ratio adjusted with 2-aminobutanol (10–100 mM) and formic acid (10–100 mM) in acetonitrile-methanol (80:20, v/v); temperature, 20 °C. log ([2-aminobutanol]/[HCOOH]) = 0 corresponds to 2-aminobutanol and formic acid each 10 mM, 1 corresponds to 100 mM 2-aminobutanol and 10 mM formic acid (basic pH* range), and −1 corresponds to 10 mM 2-aminobutanol and 100 mM formic acid (acidic pH* range). Reprinted with permission in a modified form from refs. [51,52].

mobility was obtained when the pH* of the eluent (adjusted through the acid/base ratio) was varied, and clearly indicated that the selector acidity was the dominant factor for the EOF characteristics of the particles (Fig. 15a). The weak cation exchanger (WCX) with the carboxylic acid functionality provided solely with basic pH* a strong EOF due to suppressed ionization in the acidic range. On the other hand, the sulfonic acid analog allowed the generation of a stable and high EOF over the entire pH* range. In contrast, the phosphonic acid analog exhibited unexpected behavior. EOF velocity declined in the acidic pH* range and current and flow were eventually broken down with excess of aminobutanol (basic range). It may be argued that with the bis-protic phosphonic acid the increasing charge density leads finally to excessive double layer overlap at basic pH* conditions and breakdown of the EOF. The EOF behavior of a variety of other strong sulfonic acid-based cation exchange (SCX) CSPs, some of them with an additional carboxylic acid group, is shown in Fig. 15b. It is seen that the EOF profiles are quite similar, for all of them basically dominated by the sulfonic acid functionality. Overall, the achieved EOF mobilities were quite high (μ_{eo} between 1.5×10^{-4} cm^2 V^{-1} s^{-1} and 2×10^{-4} cm^2 V^{-1} s^{-1}) despite the substantial electrolyte concentrations and strong ion-pairing properties of the aminobutanol that reduced the effective ζ-potential and EOF.

The favorable EOF characteristics of the SCX CSPs in the acidic range allowed the use of these phases at pH* conditions where non-stereoselective interactions between cationic solutes and the residual silanols of the CSPs were minimized. Noticeably, retention factors increased in the order of acidities of the CSPs (Fig. 16a) and advantageously also the separation factors as well as resolutions were enhanced on the stronger acidic cation-exchange CSPs in particular in the acidic pH* range (Fig. 16b and c) [51]. As a consequence, the SCX CSPs exhibited a broader application spectrum and allowed baseline resolutions of a wide variety of chiral bases including in particular amino alcohols like β-sympathomimetics, β-blockers, antimalarial agents, but also

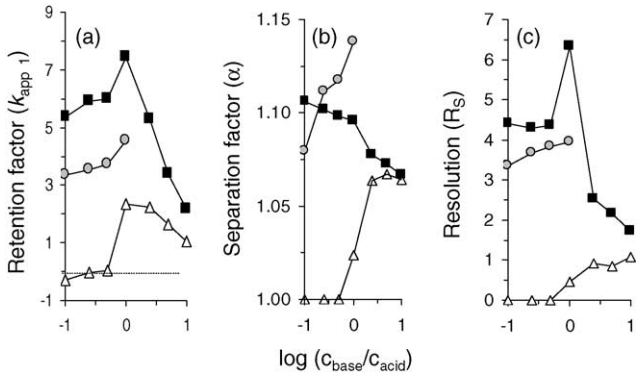

Fig. 16. pH* profiles of retention factors, enantioselectivities, and resolutions of ephedrine. CSPs: (■) sulfonic acid-based CSP 1, (◯) phosphonic acid based CSP 2, and (△) carboxylic acid based CSP 3 (for structures see Fig. 15). Same conditions as in Fig. 15. Reprinted in modified form from ref. [51].

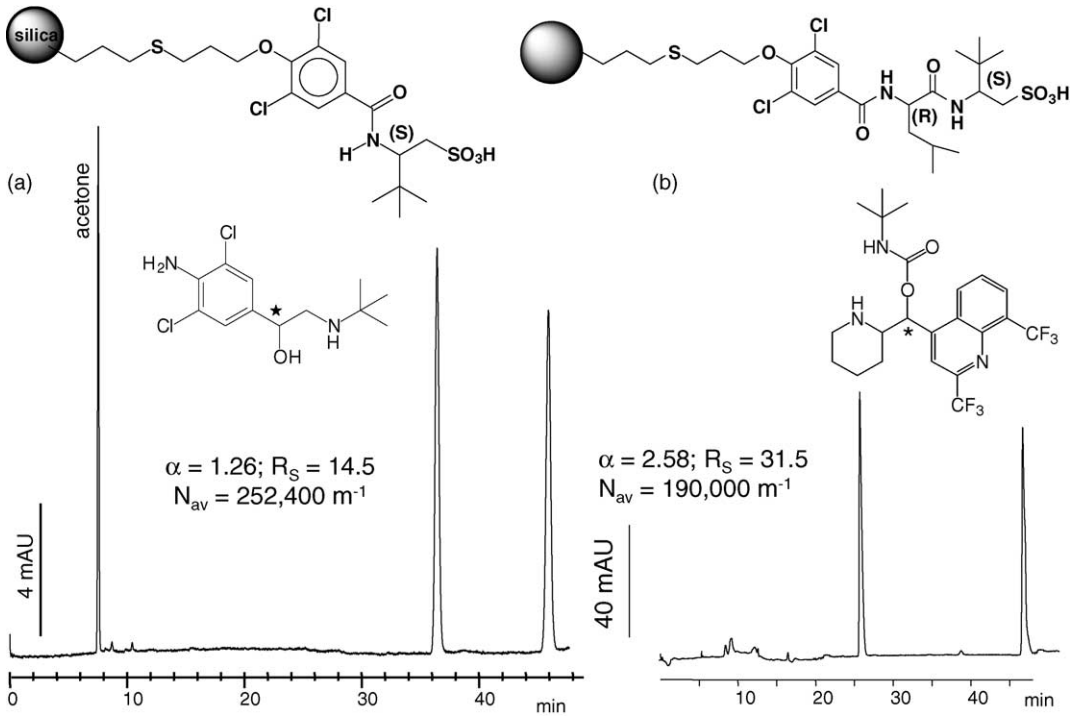

Fig. 17. Representative electrochromatograms of enantiomer separations of chiral basic compounds by NACEC on aminosulfonic acid and sulfodipeptide based SCX CSPs. (a) Clenbuterol, and (b) O-(*tert*-butylcarbamoyl)mefloquine. Column dimensions: 250 mm × 0.1 mm i.d. (L_{eff} = 250 mm, L_{tot} = 335 mm); eluent, 50 mmol/L formic acid and 25 mmol/L 2-aminobutanol in ACN–MeOH (80:20, v/v); voltage, +15 kV (18.2 μA); *T*, 20 °C. Reprinted in modified form with permission from refs. [51,54].

various non-amino alcohol structures as well as amphoteric compounds, e.g. omeprazole [51].

The various SCX CSPs presented in Fig. 14 show to some extent complementarity in terms of application spectrum which was remarkably broad in particular for the CSPs based on 2-amino-3,3-dimethylbutanesulfonic acid and corresponding dipeptides (Fig. 17). For example, the sulfodipeptide CSPs based on (S,S) and (R,S)-leucyl-2-amino-3,3-dimethylbutanesulfonic acid as selector allowed the baseline separation of about 40% of the 50 tested racemates by NACEC using a single standard mobile phase [54].

In 1995, Smith and Evans reported on CEC separations of basic pharmaceuticals using SCX particles and observed a focussing effect that yielded plate numbers in excess of a million/m [64]. This work spurred the development of CEC by attracting the interest of many researchers. Unfortunately, this focussing effect was not reproducible. In some rare cases, we could also find a similar phenomenon [51], but improper or non-optimized conditions seemed to be responsible. In order to verify whether the high efficiencies with up to 350,000 plates/m that have frequently been obtained with the sulfonic acid based-SCX CSPs, which showed better behavior in terms of peak shape and efficiencies than the phosphonic acid analogs, are artefacts or highly reproducible, a method validation was carried out for the enantiomeric excess determination of ephedrine [53]. This solute was separated on the SCX CSP based on the *N*-*tert*-butylamide of penicillamine sulfonic acid with 320,000 plates/m and R_S of 4.8. Run-to-run repeatabilities were all below 0.3% R.S.D. for EOF, retention time, separation factor, R_S and peak area ratio. The R.S.D. of about 1 was obtained for the plate numbers indicating that the separations are highly reproducible and the NACEC method of principal practical suitability. R.S.D. values of absolute peak areas were about 6.5% and hence the self-internal standard method, which makes use of the opposite enantiomer as internal standard for the quantitation of the main component, was suggested. This of course implicates that the analyses are run twice, once for the determination of the enantiomeric excess without spiking and once for the quantitation of the main enantiomer with spiking of the opposite enantiomer at a specified concentration. The self-internal standard method ensured a highly linear calibration curve (0.03–5 mg/mL; $r^2 = 0.9998$). Also the other validation issues such as LOQ (0.058% at S/N = 3:1), LOQ (0.035% at S/N = 5:1) for the minor enantiomer complied well with the requirements.

Hence, it may be concluded that this concept has exceptional potential in NACEC, in particular when the particulate support can be substituted by more robust monolithic media.

6. Conclusions

A variety of studies on enantioselective CEC have demonstrated that nonaqueous conditions may offer certain advantages over typical reversed-phase mode and hence it may be concluded that NACEC represents a distinguished complement to RP-type enantioselective CEC. Such potential advantages of NACEC include the feasibility of performing enantiomer separations of lipophilic compounds that are even insoluble in hydroorganic eluents using either the polar organic mode (MeOH-ACN based eluents) or the normal-phase (like) mode (hexane based systems with substantial amount of polar modifiers). Further, it was shown by several studies that complementary application spectra may be achieved in aqueous and nonaqueous CEC mode and therefore NACEC widened the scope of CEC. In a few studies, a better system robustness and improved baseline stability was reported, because the severe problem of bubble formation in the packed columns was largely eliminated by use of nonaqueous media. Last but not least, another striking advantage may arise from a faster elution and therefore more rapid analyses, in particular when strong hydrophobic interactions between sorbent and analytes are involved. In a few examples, it was demonstrated that NACEC can principally cope with the demands of a validated assay as, e.g. proven for the enantiomeric excess determination of enantiomeric drugs. Its principal applicability to the analysis of more complicated samples such as biological fluids has not yet been shown and its performance in this respect remains questionable. Moreover, also the coupling of NACEC to mass spectrometers is an empty spot on the landscape of this intriguing electroseparation technology. Considering that usually highly volatile solvents and electrolytes are used in NACEC it should be at least equally feasible as with aqueous CEC methods. Overall, a lot remains to be done and it is hoped that with the emergence of highly enantioselective and robust monolithic columns many of the currently existing problems can be eliminated. Indeed, the monolithic column technology could pave the way for a brighter future of enantioselective (NA)CEC. First steps seem to be done.

7. Abbreviations

Ac	acetyl
ACN	acetonitrile
AcOH	acetic acid
APS	3-aminopropylsilica
BGE	background electrolyte
Bz	benzoyl
CC	carbazole-9-carbonyl
CD	cyclodextrin
CE	capillary electrophoresis
CEC	capillary electrochromatography
Chiralcel OD	cellulose tris(3,5-dimethylphenylcarbamate)
Chiralcel OJ	cellulose tris(4-methylbenzoate)
Chiralpak AD	amylose tris(3,5-dimethylphenylcarbamate)
CLC	capillary liquid chromatography
CSP	chiral stationary phase
CySO3H-Leu	cysteic acid-leucine sulfodipeptide
DBD	4-(*N*,*N*-dimethylaminosulfonyl)-2,1,3-benzoxadiazole

DCB 3,5-dichlorobenzoyl
DEA diethylamine
DNB 3,5-dinitrobenzoyl
DNP 2,4-dinitrophenyl
Dns dansyl (5-dimethylaminonaphthalene-1-sulfonyl)
DNZ 3,5-dinitrobenzyloxycarbonyl
EDMA ethylene dimethacrylate
EOF electroosmotic flow
EtOH ethanol
FMOC-Leu *N*-(9-fluorenylmethoxycarbonyl)-leucine
FS fused silica
GMA glycidyl methacrylate
HEMA 2-hydroxyethylmethacrylate
HPLC high-performance liquid chromatography
LC liquid chromatography
LOD limit of detection
LOQ limit of quantitation
MeOH methanol
MES 2-morpholinoethanesulfonic acid
MS mass spectrometry
NACE nonaqueous capillary electrophoresis
NACEC nonaqueous electrochromatography
NMF *N*-methylformamide
NP normal-phase mode
P external pressure
PO polar organic mode
2-PrOH 2-propanol
RP reversed-phase mode
RSD relative standard deviation
SCX strong cation exchanger
TAG teicoplanin aglycone
TEA triethylamine
THF tetrahydrofuran
tBuCQN O-*tert*-butylcarbamoyl quinine
TPS 3-mercaptopropylsilica
WCX weak cation exchanger
Z benzyloxycarbonyl

List of symbols
$a_I + a_{II}$ equilibrium constant
b_I binding affinities at non-enantioselective sites I
$b_{ij,II}$ binding affinities at enantioselective sites II
$d_{channel}$ diameter of the flow channel
F Faraday constant
H theoretical plate heights
I ionic strength
k_{CEC} retention factor in CEC as calculated by LC terminology
k_{LC} purely chromatographic retention factor
L_{eff} effective length of the capillary
L_{tot} total length of the capillary
q_I saturation capacities at non-enantioselective sites I
$q_{ij,II}$ saturation capacities at enantioselective sites II
R gas constant
T absolute temperature
t_e elution time of the solute
t_0 elution time of a neutral non-retained flow marker
v_{CEC} observed migration velocity in CEC
v_{eo} EOF velocity
v_{ep} electrophoretic migration velocity
v_{press} pressurized flow velocity

Greek letters
α separation factor
α_{app} apparent chromatographic enantioselectivity
α_{CE} separation factor as calculated by electrophoretic formalism
α_{CEC} separation factor in CEC as calculated by LC terminology from k_{CEC}
α_{LC} chromatographic selectivity
α_{true} intrinsic enantioselectivity of the selector
δ double layer thickness
μ_{eo} electroosmotic mobility
μ_{ep} electrophoretic mobility
μ_r reduced mobility
σ surface charge of the chiral stationary phase
ϕ phase ratio

Acknowledgements

The financial support by the Austrian Christian Doppler Research Society and the industrial partners AstraZeneca (Södertälje, Sweden), Merck KGaA (Darmstadt, Germany) and piCHEM (Graz, Austria) is gratefully acknowledged.

References

[1] Z. Deyl, F. Svec (Eds.), Capillary electrochromatography, J. Chromatogr. Library, vol. 62, Elsevier, Amsterdam, 2001.
[2] M. Lämmerhofer, F. Svec, J.M.J. Fréchet, W. Lindner, Trends Anal. Chem. 19 (2000) 676.
[3] B. Chankvetadze, J. Sep. Sci. 24 (2001) 691.
[4] G. Gotmar, T. Fornstedt, G. Guiochon, Chirality 12 (2000) 558.
[5] S. Fanali, P. Catarcini, G. Blaschke, B. Chankvetadze, Electrophoresis 22 (2001) 3131.
[6] J. Kang, D. Wistuba, V. Schurig, Electrophoresis 23 (2002) 4005.
[7] P.J. Vickers, N.W. Smith, J. Sep. Sci. 25 (2002) 1284.
[8] X. Chen, H. Zou, M. Ye, Z. Zhang, Electrophoresis 23 (2002) 1246.
[9] D. Wistuba, K. Cabrera, V. Schurig, Electrophoresis 22 (2001) 2600.
[10] E. Tobler, M. Lämmerhofer, W. Lindner, J. Chromatogr. A 875 (2000) 341.
[11] M. Lämmerhofer, J. Chromatogr. A 1068 (2005) 3.
[12] M.M. Dittmann, K. Masuch, G.P. Rozing, J. Chromatogr. A 887 (2000) 209.
[13] C. Schwer, E. Kenndler, Anal. Chem. 64 (1991) 1801.
[14] A.S. Rathore, Electrophoresis 23 (2002) 3827.
[15] B. Sellergren, K.J. Shea, J. Chromatogr. 635 (1993) 31.
[16] E. Hilder, F. Svec, J.M.J. Fréchet, J. Chromatogr. A 1044 (2004) 3.
[17] K. Krause, B. Chankvetadze, Y. Okamoto, G. Blaschke, J. Microcol. Sep. 12 (2000) 398.
[18] I. Nischang, U. Tallarek, Electrophoresis 25 (2004) 2935.
[19] R. Stol, H. Poppe, W.T. Kok, Anal. Chem. 73 (2001) 3332.
[20] P. Catarcini, S. Fanali, C. Presutti, I. D'Acquarica, F. Gasparrini, Electrophoresis 24 (2003) 3000.
[21] E. Zarbl, Ph.D. thesis, University of Vienna, Vienna, 2001.

[22] F. Svec, T.B. Tennikova, Z. Deyl (Eds.), Monolithic materials: preparation, properties and applications, J. Chromatogr. Library, vol. 67, Elsevier, Amsterdam, 2003.
[23] T. Jiang, J. Jiskra, H.A. Claessens, C.A. Cramers, J. Chromatogr. A 923 (2001) 215.
[24] M. Lämmerhofer, W. Lindner, J. Chromatogr. A 839 (1999)167.
[25] B. Chankvetadze, Capillary Electrophoresis in Chiral Analysis, Wiley, West Sussex, 1997.
[26] B. Chankvetadze, Electrophoresis 23 (2002) 4022.
[27] K. Krause, B. Chankvetadze, Y. Okamoto, G. Blaschke, Electrophoresis 20 (1999) 2772.
[28] M. Meyring, B. Chankvetadze, G. Blaschke, J. Chromatogr. A 876 (2000) 157.
[29] M. Girod, B. Chankvetadze, G. Blaschke, J. Chromatogr. A 887 (2000) 439.
[30] M. Girod, B. Chankvetadze, G. Blaschke, Electrophoresis 22 (2001) 1282.
[31] L. Chankvetadze, I. Kartozia, C. Yamamoto, B. Chankvetadze, G. Blaschke, Y. Okamoto, Electrophoresis 23 (2002) 486.
[32] B. Chankvetadze, I. Kartozia, J. Breitkreutz, Y. Okamoto, G. Blaschke, Electrophoresis 22 (2001) 3327.
[33] M. Girod, B. Chankvetadze, Y. Okamoto, G. Blaschke, J. Sep. Sci. 24 (2001) 27.
[34] B. Chankvetadze, I. Kartozia, Y. Okamoto, G. Blaschke, J. Sep. Sci. 24 (2001) 635.
[35] B. Chankvetadze, I. Kartozia, J. Breitkreutz, M. Girod, M. Knobloch, Y. Okamoto, G. Blaschke, J. Sep. Sci. 24 (2001) 251.
[36] X. Chen, W. Jin, F. Qin, Y. Liu, H. Zou, B. Guo, Electrophoresis 24 (2003) 2559.
[37] X. Chen, F. Qin, Y. Liu, L. Kong, H. Zou, Electrophoresis 25 (2004) 2817.
[38] H. Wikström, L.A. Svensson, A. Torstensson, P.K. Owens, J. Chromatogr. A 869 (2000) 395.
[39] C. Karlsson, L. Karlsson, D.W. Armstrong, P.K. Owens, Anal. Chem. 72 (2000) 4394.
[40] S. Fanali, P. Catarcini, M.G. Quaglia, Electrophoresis 23 (2002) 477.
[41] C. Karlsson, H. Wikström, D.W. Armstrong, P.K. Owens, J. Chromatogr. A 897 (2000) 349.
[42] E. Carlsson, H. Wikström, P.K. Owens, Chromatographia 53 (2001) 419.
[43] N. Grobuschek, M.G. Schmid, J. Koidl, G. Gübitz, J. Sep. Sci. 25 (2002) 1297.
[44] E. Tobler, M. Lämmerhofer, G. Mancini, W. Lindner, Chirality 13 (2001) 641.
[45] M. Lämmerhofer, E.C. Peters, C. Yu, F. Svec, J.M. Fréchet, Anal. Chem. 72 (2000) 4614.
[46] M. Lämmerhofer, F. Svec, J.M. Fréchet, Anal. Chem. 72 (2000) 4623.
[47] M. Lämmerhofer, F. Svec, J.M.J. Fréchet, W. Lindner, J. Microcol. Sep. 12 (2000) 597.
[48] M. Lämmerhofer, E. Tobler, E. Zarbl, W. Lindner, F. Svec, J.M.J. Fréchet, Electrophoresis 24 (2003) 2986.
[49] B. Preinerstorfer, W. Bicker, W. Lindner, M. Lämmerhofer, J. Chromatogr. A 1044 (2004) 187.
[50] E. Tobler, M. Lämmerhofer, F. Wuggenig, F. Hammerschmidt, W. Lindner, Electrophoresis 23 (2002) 462.
[51] E. Zarbl, M. Lämmerhofer, A. Woschek, F. Hammerschmidt, C. Parenti, G. Cannazza, W. Lindner, J. Sep. Sci. 25 (2002) 1269.
[52] S. Constantin, W. Bicker, E. Zarbl, M. Lämmerhofer, W. Lindner, Electrophoresis 24 (2003) 1668.
[53] W. Bicker, D. Hebenstreit, M. Lämmerhofer, W. Lindner, Electrophoresis 24 (2003) 2532.
[54] D. Hebenstreit, W. Bicker, M. Lämmerhofer, W. Lindner, Electrophoresis 25 (2004) 277.
[55] L. Chankvetadze, I. Kartozia, C. Yamamoto, B. Chankvetadze, G. Blaschke, Y. Okamoto, J. Sep. Sci. 25 (2002) 653.
[56] B. Chankvetadze, G. Blaschke, Electrophoresis 21 (2000) 4159.
[57] H. Wikström, L.A. Svensson, A. Torstensson, P.K. Owens, J. Chromatogr. A (1999).
[58] O. Kornysova, P.K. Owens, A. Maruska, Electrophoresis 22 (2001) 3335.
[59] M.G. Schmid, N. Grobuschek, V. Pessenhofer, A. Klostius, G. Gübitz, Electrophoresis 24 (2003) 2543.
[60] M.G. Schmid, N. Grobuschek, V. Pessenhofer, A. Klostius, G. Gübitz, J. Chromatogr. A 990 (2003) 83.
[61] O.L.S. Muñoz, E.P. Hernández, M. Lämmerhofer, W. Lindner, E. Kenndler, Electrophoresis 24 (2003) 390.
[62] T. Fornstedt, G. Zhong, G. Guiochon, J. Chromatogr. A 742 (1996) 55.
[63] E.C. Peters, K. Lewandowski, M. Petro, F. Svec, J.M.J. Fréchet, Anal. Comm. 35 (1998) 83.
[64] N.W. Smith, M.B. Evans, Chromatographia 41 (1995) 197.